INFORMATION TO USERS

This manuscript has been reproduced from the microfilm master. UMI films the text directly from the original or copy submitted. Thus, some thesis and dissertation copies are in typewriter face, while others may be from any type of computer printer.

The quality of this reproduction is dependent upon the quality of the copy submitted. Broken or indistinct print, colored or poor quality illustrations and photographs, print bleedthrough, substandard margins, and improper alignment can adversely affect reproduction.

In the unlikely event that the author did not send UMI a complete manuscript and there are missing pages, these will be noted. Also, if unauthorized copyright material had to be removed, a note will indicate the deletion.

Oversize materials (e.g., maps, drawings, charts) are reproduced by sectioning the original, beginning at the upper left-hand corner and continuing from left to right in equal sections with small overlaps.

Photographs included in the original manuscript have been reproduced xerographically in this copy. Higher quality 6" x 9" black and white photographic prints are available for any photographs or illustrations appearing in this copy for an additional charge. Contact UMI directly to order.

ProQuest Information and Learning
300 North Zeeb Road, Ann Arbor, MI 48106-1346 USA
800-521-0600

Université d'Ottawa · University of Ottawa

STABILITY OF CERTAIN MODELS OF SUSPENSION BRIDGES

by

Hani Harbi

A thesis submitted to the
School of Graduate Studies and Research
in partial fulfillment of the requirements for the degree of

Ph.D of Applied Science

Ottawa-Carleton Institute for Electrical and Computer Engineering
School of Information Technology and Engineering
Department of Electrical and Computer Engineering
Faculty of Engineering
University of Ottawa

September, 2000

Dedication

In loving memory of my father
Mohamed Harbi Ben Ounis (1906-1992)
and my teacher Zine Dali (1945-1980)

Acknowledgements

The author expresses his deepest gratitude to his advisor Professor N.U Ahmed for his generous encouragement, invaluable guidance, and numerous hours of discussion throughout this work, without which this thesis would have not been possible.

The author would also appreciate to express his gratitude to Professor J.Z Sasiadek, Professor T. Yeap and Professor A. Lakhsassi for their acceptance to be the members of his examiners.

Special thanks are due to Dr. N. Benichou for his suggestions and discussions.

The author wishes to express his appreciation to the faculty and staff of the Department of Electrical Engineering, University of Ottawa for their kindness and support.

Financial assistance provided by the Department of Electrical Engineering of the University of Ottawa and partly from the Natural Sciences and Engineering Reasearch Council of Canada during the period of the research is gratefully acknowledged.

And finally, the author is highly indebted to his wife Louiza Harbi for her enormous patience and constant encouragement. I am also grateful to my loving mother Zohra, my aunt Nakhla, my sisters Halima and Aicha, my children Nasreddine, Sayef, Amina and Hajer.

Abstract

In this thesis the problem of stability and analysis of distributed dynamical systems with applications to engineering is considered. A methodology has been developed for rigorous modelling of suspension bridges. It was shown that the complete dynamics of the system could be described by a coupled system of hyperbolic partial differential equations. Two models (A) and (B) have been developed. These models are generalized cases of those proposed by Lazer and McKenna and that suggested by Jacober-McKenna, which includes aerodynamic forces as developed by Maurice Roseau. Stability of the system has been proved using Lyapunov's approach under different types of dynamic loading . Further the model (B) has been extended to its stochastic counter parts. Stability of suspension bridge in the presence of distributed white noise has been investigated. Also, for each loading situation, the results are illustrated by numerical simulation with physical interpretation. And finally a dynamic model of suspension bridge based on Kirchhoff plate model as road way has been presented.

Contents

List of Figures

Chapter 1

Introduction

1.1 General

Suspension bridges have a history of large-scale oscillations that may lead to a catastrophic failure under high and even moderate forces such as wind, earthquake or traffic. Many people have seen the dramatic large-scale oscillations, followed by the collapse of the Tacoma Narrows suspension bridge. In the report on the destruction of the Tacoma Narrows bridge, eye-witnesses describe vertical and torsional motion of the bridge [Figure 1.1]. As a result of these oscillations, the cables started to loosen and tighten, producing a nonlinear effect. Some other bridges have also exhibited vibration problems. The Bronx-Whitestone bridge, on which a traveller might often get seasick due to the large-scale motions, or the Golden Gate Bridge, which has exhibited travelling waves, had exhibited oscillatory behaviour due to the action of wind.

The cause and nature of the vertical and torsional oscillations can be studied by considering a simple model of a suspension bridge. Researchers such as Lazer and McKenna [10] have found that the bridge behaves like a particle of mass one at the end of a spring with spring constant, k, which is subject to a forcing term of frequency $\mu/2\pi$. If μ is very close to the square root of k, the frequency just happened to be at a value very close

to a resonant frequency of the bridge, i.e., large oscillations occur. Thus, even though the magnitude of the forcing term was small, the phenomenon of linear resonance was enough to explain the large oscillations and eventual collapse of the bridge.

In addition, it should be emphasized that because of the observed torsional motion, some of the cables were alternately loosening and tightening. This is the nonlinear effect which requires further study. Moreover, the restoring force due to a cable is such that it strongly resists expansion, but does not resist compression. Therefore, fundamental nonlinearity is very distinctive and should be considered in any dynamic analysis.

From an overview of what was said thus far, there is a need to give a clear and simple mathematical argument as to why suspension bridges oscillate and find the effect of nonlinearity behaviour of their cables.

1.2 Literature Review

The problem of vibration of suspension bridges have been studied since 1920. Many researchers proposed different solutions and the following paragraphs describe some of the research related to the problem treated in this thesis.

The federal works agency report [1] by Amann, Von Karman and Woodruff, on the collapse of the Tacoma Narrows bridge in the State of Washington on November 7, 1940, as a result of wind action, created a widespread demand from both the general public and the engineering profession that steps be taken to inaugurate a comprehensive investigation of the problem of dynamic oscillation in suspension bridges, with a view to understand the causes of such destructive oscillations and develop design techniques to prevent their recurrence in future. The Advisory Board on the investigation of suspension bridges undertook the following objectives:

- To determine the causes and the phenomenon of vibration in suspension bridges.
- To correlate and develop a rational theory explanatory of the phenomenon of vibration.
- To create new methods of design practice, applicable to future bridges.

Following the tragedy of the Tacoma Narrows bridge, a number of researchers, including Bleich, McCullough, Rosecrans, and Vincent [2], Wiles [3], Selberg [4], Abdel-Ghaffer [5] and Lazer and McKenna [10] started seriously studying the mathematical theory of vibration of suspension bridges.

Abdel-Ghaffar [5] gave a new methodology of free vibration analysis of suspension bridge with horizontal decks, utilizing a continuum approach to include the coupling between the vertical and torsional vibration and the effects of cross-sectional distortion. Variational principles were used to obtain the coupled equations of motion in their most general and nonlinear form.

Kawada and Hirai [6] examined a new approach through mathematical analysis and wind tunnel test to suspension bridge rehabilitation. They studied the relationship between the suspended mass and the limited oscillations of the long span suspension bridges. On the basis of their work, they put together the following conclusions:

- Suspension bridges demand the right amount of mass, otherwise, the result of oscillations will be disastrous and will charge an expensive compensation.
- If suspension bridges, with stream-lined stiffening girder, had any troubles, their cause must be mainly due to the lack of mass.

In [7], McKenna and Walter investigated nonlinear oscillations in a suspension bridge, where the model was suggested by Lazer and McKenna [8]. As a model of suspension bridge they consider a one-dimensional beam of length L suspended by cables. When the cables are stretched, there is a restoring force which is assumed to be proportional to the amount

of the stretching (Hooke's law). But when the beam moves in the opposite direction, then there is no restoring force exerted on it.

Oscillation induced fatigue of the structural members is a major factor limiting the useful life of a suspension bridge. Some relevant studies regarding oscillatory solutions were carried out by [9].

In reference [10], Lazer and McKenna studied the problem of nonlinear oscillation in a suspension bridges. They presented a one-dimensional mathematical model for the bridge, that takes account of the fact that the coupling provided by the stays connecting the suspension (main) cable to the deck of the road bed is fundamentally nonlinear.

McKenna and Walter [11] considered the existence of travelling wave solutions to a nonlinear beam equation which was proposed as a model for a suspension bridge in two previous articles [7] and [8].

In reference [12], a theory has been advanced which describes the one-dimensional vertical oscillation in suspension bridge, and which shows the behaviour of the following items:

- Suspension bridges are prone to large-scale oscillation;
- The occurrence of this large-scale oscillation is dependent on initial conditions;
- Large vertical oscillations can rapidly change, virtually instantaneously to torsional two-dimensional oscillations;
- The torsional oscillation was not of a single nodal type, but changed from no-noded to one-noded and back, both types of motion having the same period but with the no-noded motion having somewhat larger amplitude;
- Sometimes the torsional oscillation would be bigger at one end, indicating some asymmetry in the motion.

Jacover and McKenna [13] gave some explanation of why a nonlinearly suspended beam,

subject to periodic forcing, could exhibit large-scale oscillations of a torsional type or, under the same periodic forcing term, could exhibit small linear torsional oscillations about equilibrium. The authors came up with the following conclusions:

- The long-term response to any given forcing term is highly sensitive to the initial conditions.
- In the presence of vertical forcing terms, the multiple-solution behaviour seems to be purely vertical.

Billah and Scanlan [15] have pointed aerodynamic self-excitation behavior that was able to impart a net negative damping to the system as in flutter which accounts for the destructive behavior of the bridge .

Recently rigorous analysis of suspension bridge based on the PDE models (Deterministic as well as Stochastic) and their stability issues were performed [16,18-22]. As well, some mathematical analysis of dynamic (PDE) models of suspension bridges as proposed by Lazer and McKenna as described in [10] was presented [16].

In [19] the asymptotic stability, in particular exponential stability of the structure with reference to the aerodynamic and structural damping was mainly studed. This is practically important since a suspension bridge taking long time to settle down to its rest state in not desirable. However these studies do not include the torsional motion. In a later work, Jacover and McKenna [13] presented a model that includes torsional motion. However a complete analysis of the system was not included. In [21] Jacover-McKenna model with the model for aerodynamic forces as developed in the book by Maurice Roseau [14] was used and a complete mathematical analysis was presented. Finaly stability of torsional and vertical motion of suspension

bridges subject to random wind forces was considered [22]. The results are also illustrated by numerical simulation along with the physical interpretation and discussions thereof.

In addition to the vibration and oscillation of suspension bridges, which are typically a structural domain problems, instability and vibration problems are also encountered in space structures such as communication satellites, space shuttle and space station which are equipped with large antennas mounted on long flexible masts that could be modelled as beams [23-26]. These problemd can be solved in similar fashion as the suspension bridge.

It is expected that this study will have useful engineering application in design and analysis of suspension bridges located in the regions of high seismic or wind loads.

1.3 Thesis Objectives and Contributions

This thesis presents a refinement of the models proposed by Laser and McKenna as described in [10] and that suggested by Jacover-McKenna in [13], which includes aerodynamic forces as developed in the book by Maurice Roseau [14]. The explicit objectives of this study can be outlined as follows:

- A presentation of the Partial Differential Equations (PDE) version of the Laser-McKenna suspension bridge model.
- A presentation of two dynamic models of suspension bridges described by a system of hyperbolic parial differential equations with linear and nonliear couplings.
- The stability properties of these models and the relative effectiveness of aerodynamic and structural damping have been studied analytically. Furtheir the impact of the wind forces in presence and absence of aerodynamic and strutural damping on the stability motion of the second system was also stued.
- A presentation of a stochastic version of the model (B) and analysis of its dynamic under

stochastic loading.

• A presentation of a dynamic model of suspension bridge based on Kirchhoff plate model as road way.

• An illustration of the numerical results from the models simulating the physical interpretation.

Outline of the thesis

- Motivation
- Dynamic Models of Suspension Bridge and Their Stability
- Modelling of Torsional and Longitudinal Vibration of Suspension Bridge Subject to Aerodynamic Forces
- Stochastic Modelling and Stability of Suspension Bridge
- Plate Model For Suspension Bridge
- Conclusions and Suggestions for Further Research
- References

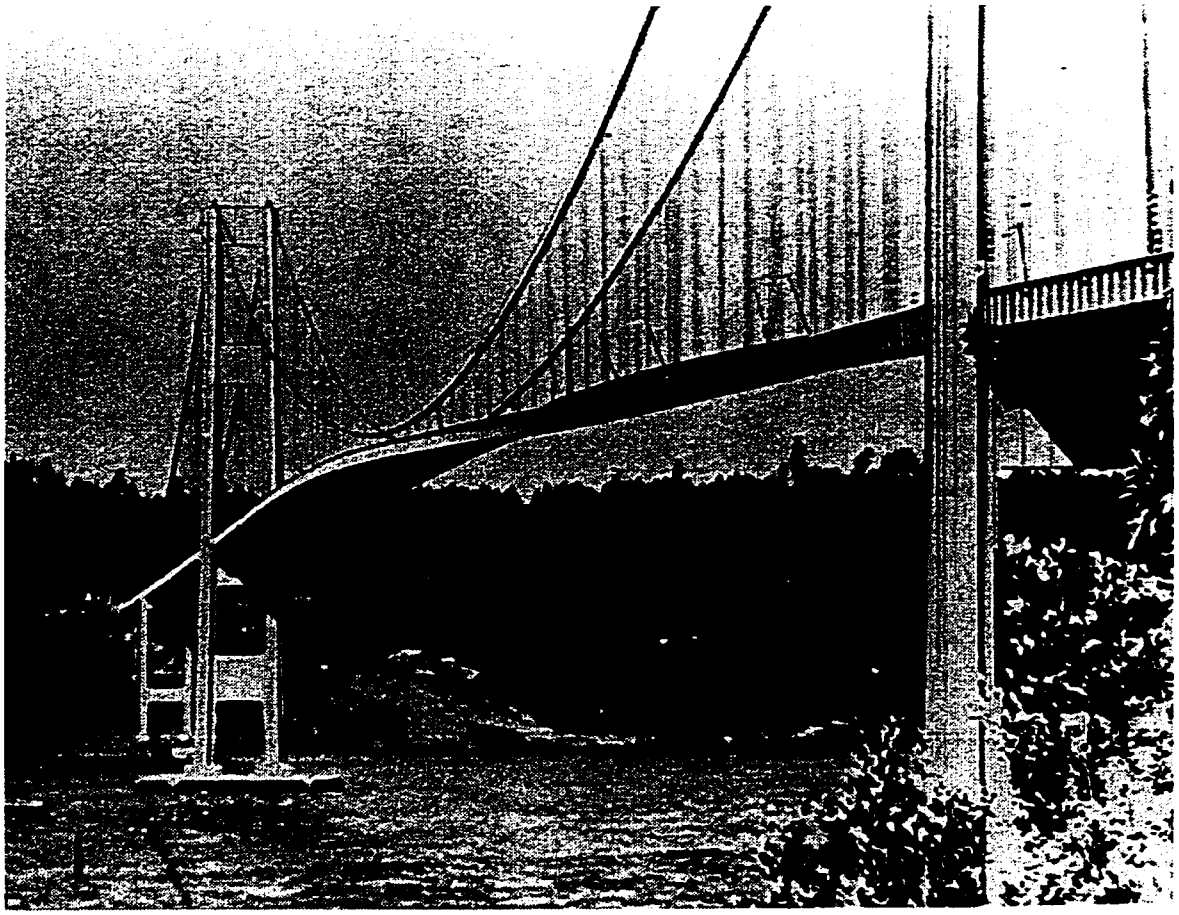

Figure 1.1:Torsional motion of the Tacoma Narrows Bridge just before failure, November 7, 1940. (*Courtesy Special Collections Division, University of Washington Libraries. Photo by F. B. Farquharson [negative No. 4].*)

Chapter 2

Dynamic Models of Suspension Bridge and Their Stability

2.1 General

In this chapter a few dynamic models of suspension bridges described by partial differential equations with linear and nonlinear couplings are presented. The stability properties of these models and the relative effectiveness of aerodynamic and structural damping have been studied analytically . This study shows that increasing either of these damping coefficients indefinitely does not necessarily increase the decay rate indefinitely. In view of possible disastrous effects of high wind, structural damping is preferable to viscous damping. These results are illustrated by numerical simulation. For clarity of the method, a simple suspension bridge configuration is considered in Figure 2.1.

2.2 Some Relevant Function Spaces

Before going into the details of the modelling, it is worthwile establishing some relevant function spaces. These functions spaces will be used for the development of the models and the analysis of their solutions.

Let $\Sigma \subset R^n$ be an open bounded set with smooth boundary $\partial\Sigma$ and let

$$L_2(\Sigma) = \left\{ v | \int_\Sigma |v|^2 dx = ||v||^2_{L_2(\Sigma)} < \infty \right\}$$

denote the space of equivalence classes of Lebesgue square integrable functions with the standard norm topology. Let $H^m(\Sigma) \equiv H^m, \quad m \in N$, denote the standard Sobolev space with the usual norm topology

$$||\psi||_{H^m} \equiv \sum_{|\alpha| \leq m} ||D^\alpha \psi||_{L_2(\Sigma)},$$

where

$$D^\alpha \psi = \frac{\partial^{|\alpha|}\psi}{\partial x_1^{\alpha_1} ... x_n^{\alpha_n}}, \quad |\alpha| = \alpha_1 + \alpha_2 + ... + \alpha_n, \ \alpha_i \geq 0,$$

and $H_0^m(\Sigma) \equiv H_0^m \subset H^m$ denote the completion in the topology of H^m of C^∞ functions on Σ with compact support. From classical results on Sobolev spaces it is well known that the elements of H_0^m are those of H^m which, along with their conormal derivatives up to order $m-1$, vanish on the boundary $\partial\Sigma$. The dual of H_0^m is H^{-m} which is a subspace of the space of distributions $\mathcal{D}'(\Sigma)$. The reader will find more details about Sobolev spaces in references like Lions-Magenes [42], Nečas [43] or Adams [17].

2.3 Model (A) (Vertical Motion):

A simplified model of a suspension bridge such as the one shown in Figure 2.1, is given by a coupled systems of partial differential equations, taken from Lazer and McKenna [10] of the form :

$$\begin{cases} m_b \dfrac{\partial^2 z}{\partial t^2} + \alpha_b \dfrac{\partial^4 z}{\partial x^4} - F_0(y-z) = m_b g + f_1, \quad x \in (0, L) \equiv \Sigma, \quad t \geq 0, \\ m_c \dfrac{\partial^2 y}{\partial t^2} - \alpha_c \dfrac{\partial^2 y}{\partial x^2} + F_0(y-z) = m_c g + f_2, \quad x \in (0, L) \equiv \Sigma, \quad t \geq 0, \end{cases} \tag{2.1}$$

The first equation describes the vibration of the road bed in the vertical plane and the second equation describes that of the main cable from which the road bed is suspended by stays cables. $\frac{\partial^k}{\partial x^k}$ denotes the spatial derivative of order k. Here m_b, m_c are the masses per unit length of the road bed and the cable respectively; α_b and α_c are the flexural rigidity of the structure and coefficient of tensile strength of the cable, respectively.

The function F_0 given by

$$F_0(\xi) = \begin{cases} \xi & \text{if } \xi > 0 \\ \\ 0 & \text{otherwise} \end{cases}$$

represents the restraining force experienced both by the road bed and the suspension cable as transmitted through the tie lines (stays) thereby producing the coupling between the two. The functions f_1 and f_2 represent external as well as nonconservative forces generally time dependent.

2.3.1 Static Load:

Letting all time derivatives equal to zero in (2.1), the equations of motion becom

$$\begin{cases} \alpha_b \dfrac{\partial^4 z_s}{\partial x^4} - F_0(y_s - z_s) = m_b g, \quad x \in (0, L) \equiv \Sigma, \\ \\ -\alpha_c \dfrac{\partial^2 y_s}{\partial x^2} + F_0(y_s - z_s) = m_c g, \quad x \in (0, L) \equiv \Sigma. \end{cases} \tag{2.2}$$

where z_s, y_s satisfy the system (2.2) as shown in [16].

Subtracting equation (2.2) from (2.1) we obtain the following system of equations

$$\begin{cases} m_b \dfrac{\partial^2 \tilde{z}}{\partial t^2} + \alpha_b \dfrac{\partial^4 \tilde{z}}{\partial x^4} - F(\tilde{y} - \tilde{z}) = f_1, \quad x \in \Sigma \equiv (0, L), \quad t \geq 0, \\ m_c \dfrac{\partial^2 \tilde{y}}{\partial t^2} - \alpha_c \dfrac{\partial^2 \tilde{y}}{\partial x^2} + F(\tilde{y} - \tilde{z}) = f_2, \quad x \in \Sigma \equiv (0, L), \quad t \geq 0, \end{cases} \tag{2.3}$$

where $\tilde{z} \equiv z - z_s$, $\tilde{y} \equiv y - y_s$ and the function F is given by

$$F(\tau) \equiv F_0(\tau + z_s - y_s) - F_0(z_s - y_s)$$

For the rest of the chapter an assumption is made that the displacements is denoted by z, y instead of $\tilde{z}$, $\tilde{y}$. The system of equations (2.3) is used as the general model.

2.4 Boundary and Initial Conditions

Assuming that the deck is clamped at both ends the boundary conditions are given by

$$\begin{cases} z(t, 0) = z(t, L) = 0, \quad \dfrac{\partial z}{\partial x}(t, 0) = \dfrac{\partial z}{\partial x}(t, L) = 0 \\ y(t, 0) = y(t, L) = 0. \end{cases} \tag{2.4}$$

In case it is hinged at both ends the boundary conditions are given by

$$\begin{cases} z(t, 0) = z(t, L) = 0, \quad \dfrac{\partial^2 z}{\partial x^2}(t, 0) = \dfrac{\partial^2 z}{\partial x^2}(t, L) = 0 \\ y(t, 0) = y(t, L) = 0. \end{cases} \tag{2.5}$$

Other combinations, such as hinged on one side and clamped on the other, are also used. The initial conditions are given by

$$\begin{cases} z(0,x) = z_0(x), \quad \dfrac{\partial z}{\partial t}(0,x) = z_1(x), \quad x \in (0,L) \equiv \Sigma \\ \\ y(0,x) = y_0(x), \quad \dfrac{\partial y}{\partial t}(0,x) = y_1(x), \quad x \in (0,L) \equiv \Sigma \end{cases} \tag{2.6}$$

where z_0, z_1, y_0, y_1 are suitable real valued functions defined on $\Sigma = (0, L)$. Using Fadeo-Galerkin method one can establish the existence and uniqueness of solutions of the system (2.3) to (2.6), (see [16]). Given that $z_0 \in H_0^2$, $z_1 \in L_2(\Sigma)$, $y_0 \in H_0^1$ and $y_1 \in L_2(\Sigma)$, the systems (2.3) to (2.6) have unique solutions $\{z, y\} \in L_\infty(I, H_0^2 \times H_0^1)$ and

$$\left\{\frac{\partial z}{\partial t}\ ,\ \frac{\partial y}{\partial t}\right\} \in L_\infty(I, L_2(\Sigma) \times L_2(\Sigma)).$$

2.5 Stability

In this section, the stability of suspension bridge described by the coupled system of hyperbolic partial differential equations (2.1) along with the boundary conditions (2.4) to (2.5) has been studied .

Model (A) : First the model (A) given by the system (2.1) have been considered. In general the function F of the system (2.3) can be taken as any function with its graph lying in the first and third quadrant of the plane R^2. However from a physical point of view, it makes sense only if F is nondecreasing function of its argument. If $F(\xi) = K\xi$, the system is linear. But if

$$F(\xi) = \begin{cases} K\xi & \text{if } \xi > 0 \\ \\ 0 & \text{otherwise} \end{cases}$$

the system is nonlinear, where the quantity K denotes the stiffness coefficient of the stays connecting the road bed to the suspension cable. This situation arises whenever there is loss

of tension in the vertical cables. In any case for the general problem, let us consider the corresponding homogeneous system:

$$\begin{cases} m_b \dfrac{\partial^2 z}{\partial t^2} + \alpha_b \dfrac{\partial^4 z}{\partial x^4} - F(y-z) = 0, \quad x \in \Sigma \equiv (0,L), \quad t \geq 0, \\ m_c \dfrac{\partial^2 y}{\partial t^2} - \alpha_c \dfrac{\partial^2 y}{\partial x^2} + F(y-z) = 0, \quad x \in \Sigma \equiv (0,L), \quad t \geq 0. \end{cases} \tag{2.7}$$

This is subject to the same set of boundary and initial conditions as in (2.4) - (2.5) and (2.6) respectively. For simplicity we denote by:

$$G(\zeta) \equiv \int_0^{\zeta} F(\xi) d\xi.$$

The total system energy function is defined as a measure of vibration of the bridge with respect to the vertical plane and is then given by

$$E(t) \equiv (1/2) \int_0^L \left\{ m_b \left| \frac{\partial z}{\partial t} \right|^2 + m_c \left| \frac{\partial y}{\partial t} \right|^2 + \alpha_b \left| \frac{\partial^2 z}{\partial x^2} \right|^2 + \alpha_c \left| \frac{\partial y}{\partial x} \right|^2 + 2G(y-z) \right\} dx \tag{2.8}$$

Where the Lyapunov function defined in equation (2.8) actually represents the total energy of the general nonlinear system. The integration of the first and the second terms in (2.8) represents the kinetic energy of the roadway and the main cables respectively and that of the third and forth terms represents the potential energy of the roadbed and the main cables respectively. Finally the integration of the last term in (2.8) represents the elastic-potential energy in the stays cables .

In what follows we compute the derivative of the Lyapunov function $E(t)$ with respect to time. For simplicity we denote by:

$$\Gamma(t) = \int_0^L 2G(y-z) dx$$

it is not difficult to verify that

$$\begin{aligned}
\frac{d\Gamma(t)}{dt} &= \int_0^L \frac{\partial}{\partial t} 2G(y-z)dx \\
&= 2\int_0^L \frac{\partial}{\partial t} G(y-z)dx \\
&= 2\int_0^L G'(y-z)\left(\frac{\partial y}{\partial t} - \frac{\partial z}{\partial t}\right)dx \\
&= 2\int_0^L F(y-z)\left(\frac{\partial y}{\partial t} - \frac{\partial z}{\partial t}\right)dx
\end{aligned}$$

then

$$\begin{aligned}
\frac{dE(t)}{dt} &= (1/2)\int_0^L \left\{2m_b\left(\frac{\partial z}{\partial t}\frac{\partial^2 z}{\partial t^2}\right) + 2m_c\left(\frac{\partial y}{\partial t}\frac{\partial^2 y}{\partial t^2}\right) + 2\alpha_b\left(\frac{\partial^2 z}{\partial x^2}\left(\frac{\partial^2}{\partial x^2}\left(\frac{\partial z}{\partial t}\right)\right)\right)\right\}dx \\
&+ (1/2)\int_0^L \left\{2\alpha_c\left(\frac{\partial y}{\partial x}\left(\frac{\partial}{\partial x}\left(\frac{\partial y}{\partial t}\right)\right)\right)\right\}dx + (1/2)(d/dt)\Gamma(t)
\end{aligned}$$

After integration by parts and using the system (2.7) along with the boundary conditions (2.4) or (2.5) on can obtain:

$$\frac{dE(t)}{dt} = \int_0^L \left\{\left(m_b\frac{\partial^2 z}{\partial t^2} + \alpha_b\frac{\partial^4 z}{\partial x^4} - F(y-z)\right)\frac{\partial z}{\partial t} + \left(m_c\frac{\partial^2 y}{\partial t^2} + \alpha_c\frac{\partial^2 y}{\partial x^2} + F(y-z)\right)\frac{\partial y}{\partial t}\right\}dx$$

Since $\{z, y\}$ is the solution of the systems (2.4) to (2.7), it follows from (2.7) and the above expression that $\frac{dE}{dt} = 0$ and hence

$$E(t) = E(0), \quad \text{for all} \quad t \geq 0$$

This shows that the nonlinear system (2.4) to (2.7) is conservative and hence stable in the Lyapunov sens.

In view of the above results it is observed that in the absence of external forces. a suspension bridge linear or nonlinear model is conservative. also for more details see [33].

Remark 2.1

The interchange of energy between the main cables and the roadbed through the stays lines leads to change the deflection of the system and the amplitude of vibration of the roadway. The above results can be summarized as a theorem:

Theorem 2.1

In the absence of external forces a suspension bridge, linear or nonlinear, is conservative. The total energy functionals given by (2.8) for the model (A) is Lyapunov function for the system (2.3) and hence it is stable in the Lyapunov sense.

From engineering point of view Lyapunov stability is not good enough. and one must have asymptotic stability with reasonable satisfactory decay rate. This stability is studied in the following section.

2.6 Asymptotic Stability

However the system (2.7) is not asymptotically stable with respect to the rest state though this is what is desirable for engineering structures.

2.6.1 Aerodynamic vs Structural Damping:

In all the models given above aero-dynamic damping has been neglected. The addition of damping represents more the practical case of suspension bridge. Considering the model (A) given by (2.3) and including aerodynamic damping, it can be written as :

$$\begin{cases} m_b \dfrac{\partial^2 z}{\partial t^2} + \alpha \dfrac{\partial^4 z}{\partial x^4} - F(y-z) + f_1\left(\dfrac{\partial z}{\partial t}\right) = 0, \quad x \in (0, L), \quad t \geq 0; \\ m_c \dfrac{\partial^2 y}{\partial t^2} - \beta \dfrac{\partial^2 y}{\partial x^2} + F(y-z) + f_2\left(\dfrac{\partial y}{\partial t}\right) = 0, \quad x \in (0, L), \quad t \geq 0 \end{cases} \tag{2.9}$$

This is subject to the same set of boundary and initial conditions as in (2.4) - (2.5) and (2.6) respectively. Using the energy function (2.8) and carrying out the differentiation one can verify that

$$\frac{dE(t)}{dt} = \int_0^L \left\{ f_1\left(\frac{\partial z}{\partial t}\right)\frac{\partial z}{\partial t} + f_2\left(\frac{\partial y}{\partial t}\right)\frac{\partial y}{\partial t} \right\} dx \tag{2.10}$$

It follows from this expression that if $f_i(\xi)\xi \leq 0$ then $\dot{E} \leq 0$. Here a result similar to that of LaSalle invariance is needed to conclude that the system is asymptotically stable with respect to the rest state, given that $f_i(0) = 0, \quad f_i(\zeta)\zeta < 0, \text{ for } \zeta \neq 0. \quad \text{and } F(\xi)\xi \geq 0. \text{ for } \xi \in R.$

To prove the stability of the studied system the following theorem is considered:

Theorem 2.2

Consider the system (2.10) and suppose the following assumptions hold:

- $f_i(0) = 0, \quad f_i(\zeta) < 0, \text{ for } \zeta \neq 0,$
- $F(\xi)\xi \geq 0, \text{ for } \xi \in R.$

Then the system is asymptotically stable with respect to the rest state (zero state). For detailed proof see [16].

This stability property also holds for linear aerodynamic damping with

$$f_1(\xi) = -\gamma_1 \xi, \qquad f_2(\xi) = -\gamma_2 \xi.$$

In this case equation (2.11) reduces to

$$\frac{dE(t)}{dt} = -\int_0^L \left\{ \gamma_1 \left| \frac{\partial z}{\partial t} \right|^2 + \gamma_2 \left| \frac{\partial y}{\partial t} \right|^2 \right\} dx, \tag{2.11}$$

where γ_1 , $\gamma_2 > 0$, are the aerodynamic (or viscous damping) coefficients of the road bed and the main cables respectively. The constantes $\{\gamma_1$, $\gamma_2\}$ are dependent.

One can not indefinitely increase the viscous damping. Further it is not desirable since wind actions can destabilize the bridge. In this case it is desirable to use smart materials having good structural damping. The fact that increasing aerodynamic damping does not increase the decay rate, this was demonstrated theoretically in [19] and here numerical evidence is presented.

2.6.2 Combined Structural and Viscous Damping for Model (A)

In the presence of both viscous and structural damping, f_1 is a function of both termes

$$\frac{\partial z}{\partial t}, \ \frac{\partial^2}{\partial x^2}\left(\frac{\partial z}{\partial t}\right) \equiv \frac{\partial}{\partial t}\left(\frac{\partial^2 z}{\partial x^2}\right) \text{ and possibly } \frac{\partial^4}{\partial x^4}\left(\frac{\partial z}{\partial t}\right).$$

Assuming linearity f_1 may be given by

$$f_1\left(\frac{\partial z}{\partial t}, \frac{\partial^2}{\partial x^2}\left(\frac{\partial z}{\partial t}\right), \frac{\partial^4}{\partial x^4}\left(\frac{\partial z}{\partial t}\right)\right) = -\gamma_1\left(\frac{\partial z}{\partial t}\right) + \gamma_{12}\frac{\partial^2}{\partial x^2}\left(\frac{\partial z}{\partial t}\right) - \gamma_{13}\frac{\partial^4}{\partial x^4}\left(\frac{\partial z}{\partial t}\right).$$

For the suspension cable, structural damping is negligible. Assuming linear viscous damping f_2 is given by

$$f_2\left(\frac{\partial y}{\partial t}\right) = -\gamma_2\left(\frac{\partial y}{\partial t}\right).$$

Clearly from physical consideration γ_1, γ_{12}, $\gamma_2 \geq 0$. Substituting f_1 and f_2 in equation (2.11), we can writte

$$\frac{dE(t)}{dt} = -\int_0^L \left\{ \gamma_1 \left| \frac{\partial z}{\partial t} \right|^2 + \gamma_{12} \left| \frac{\partial}{\partial x}\left(\frac{\partial z}{\partial t}\right) \right|^2 + \gamma_{13} \left| \frac{\partial^2}{\partial x^2}\left(\frac{\partial z}{\partial t}\right) \right|^2 + \gamma_2 \left| \frac{\partial y}{\partial t} \right|^2 \right\} dx \leq 0. \tag{2.12}$$

From (2.13) one can justify that the system is asymptotically stable with respect to the origin.

Remarque 2.2

In the presence of both aerodynamic and structural damping, a suspension bridge, linear or nonlinear, is asymptotically stable in Lyapunov sens and the decay rate can be optimized by suitable choice of the coefficients.

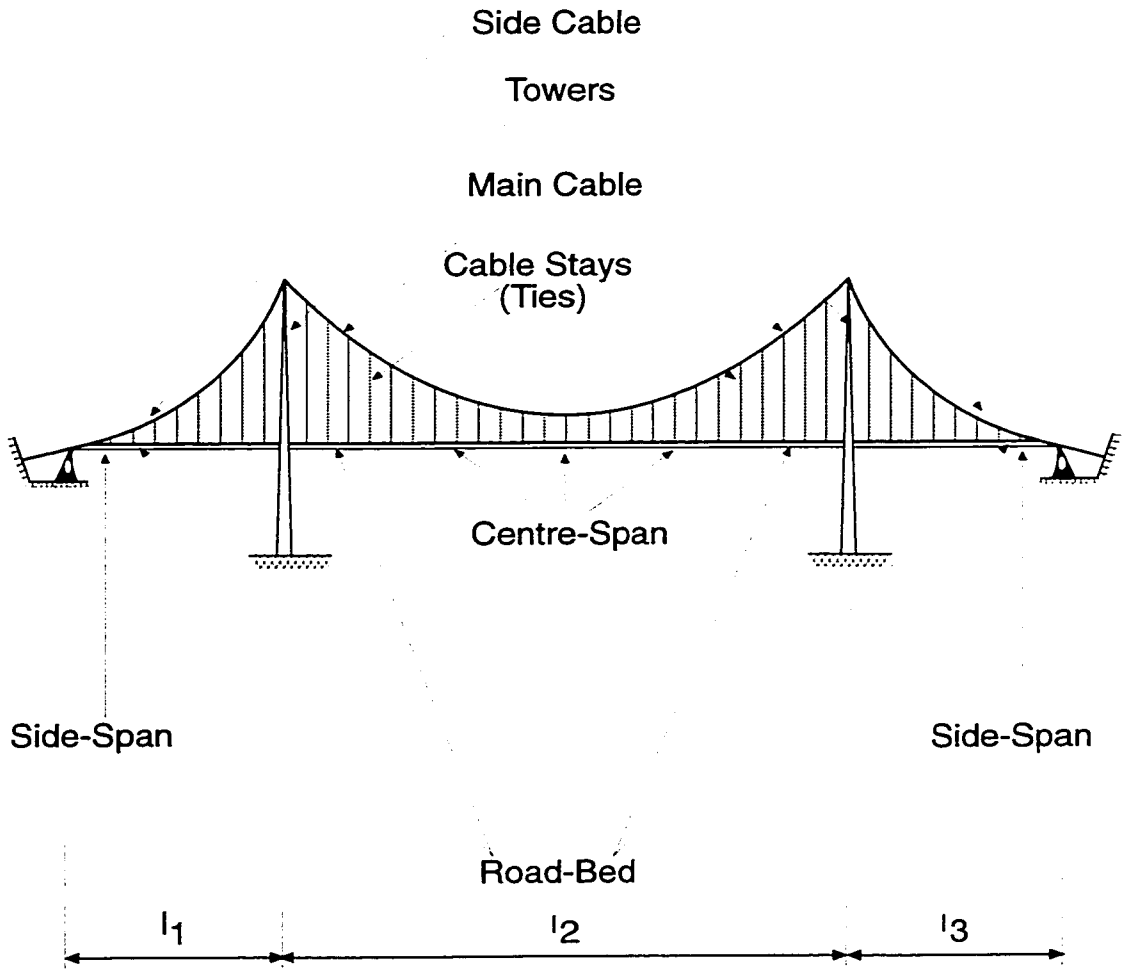

Figure 2.1: General Definition Diagram of Suspension Bridge

2.7 Numerical Results and Discussions

This section presents some simulation results and discussions from a direct application of the developed model (A) . The simulations are related to the typical suspension bridge shown in Figure 2.1. The problem was solved by finite-difference method utilizing central-difference approximations [29] and [30]. The size of time steps and space steps that are used, have been found to be sufficiently small to give highly accurate and stable solutions ($\frac{\Delta t}{\Delta x} = 2.10^{-3}$). For the purpose of simulation, the road bed and the cables are assumed to be uniform. The data used for the simulation is listed as follows:

$$m_b = 10. \quad m_c = 1. \quad k = 100. \quad \alpha = 10. \quad \beta = 1$$

In view of the above results, designers can must try to provide sufficient damping so as to obtain fast dissipation of energy. This will reduce the risk of failure due to fatigue caused by sustained oscillation.

The simulation results indicating the effectiveness of the two processes of damping have been presented. In general according to equations (2.8)-(2.9) it is evident that in the absence of any damping, aerodynamic or structural, a suspension bridge is conservative. This is given by the total energy plots as shown in the figures by the (flat) graph (a) in all the figures. The damping parameters used for each of the cases a, b, c, d, e are shown in the graphs with the first column giving the values of damping coefficients γ_1 for the road bed, the second entry γ_2 giving those for the main cables and the third giving the values of structural damping $\gamma_{1,2}$ of the road bed. Figures 2.2(a) for linear and 2.2(b) for nonlinear systems, give energy plots for increasing viscous damping coefficients; figures 2.2(c) (linear) and 2.2(d) (nonlinear) give the energy plots for increasing structural damping coefficients. Figures 2.3(a) (linear) and 2.3(b) (nonlinear) give energy plots for increasing structural damping coefficients corresponding to a fixed optimum viscous damping.

	γ_1	γ_2	γ_{12}
a:	0	0	0
b:	10^{-5}	0	0
c:	10^{-4}	0	0
d:	10^{-3}	0	0
e:	10^{-2}	0	0

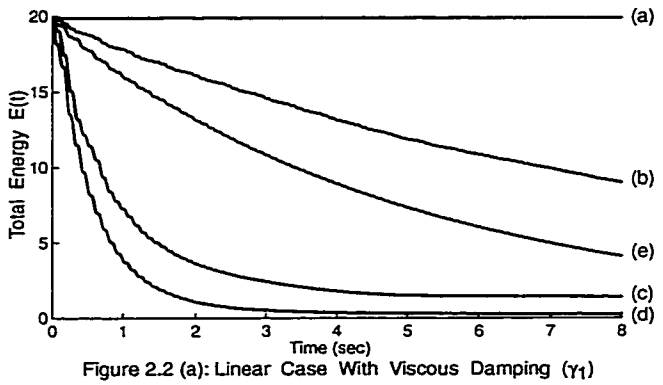

Figure 2.2 (a): Linear Case With Viscous Damping (γ_1)

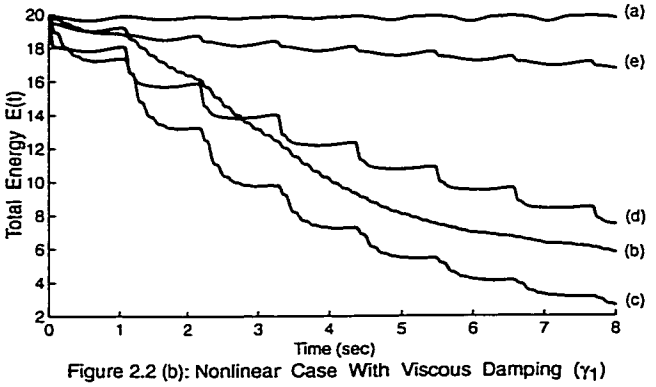

Figure 2.2 (b): Nonlinear Case With Viscous Damping (γ_1)

Time (sec)

	γ_1	γ_2	γ_{12}
a:	0	0	0
b:	0	0	10^{-5}
c:	0	0	10^{-4}
d:	0	0	10^{-3}
e:	0	0	10^{-2}

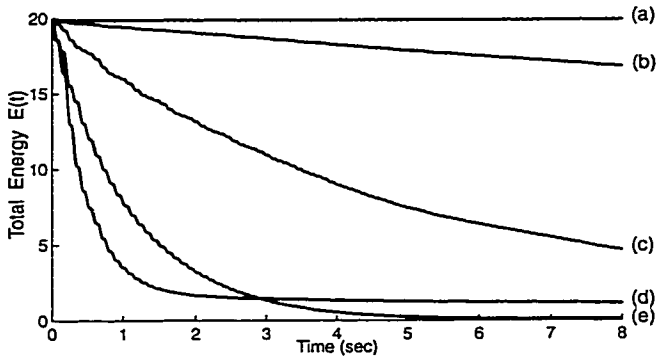

Figure 2.2 (c): Linear Case With Structural Damping (γ_{12})

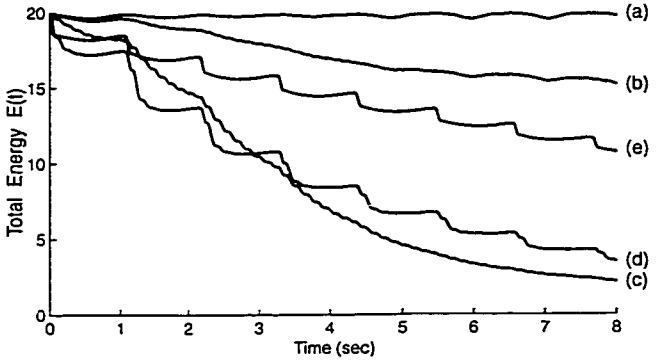

Figure 2.2 (d): Nonlinear Case With Structural Damping (γ_{12})

	γ_1	γ_2	γ_{12}
a:	0	0	0
b:	10^{-3}	0	10^{-5}
c:	10^{-3}	0	10^{-4}
d:	10^{-3}	0	10^{-3}
e:	10^{-3}	0	10^{-2}

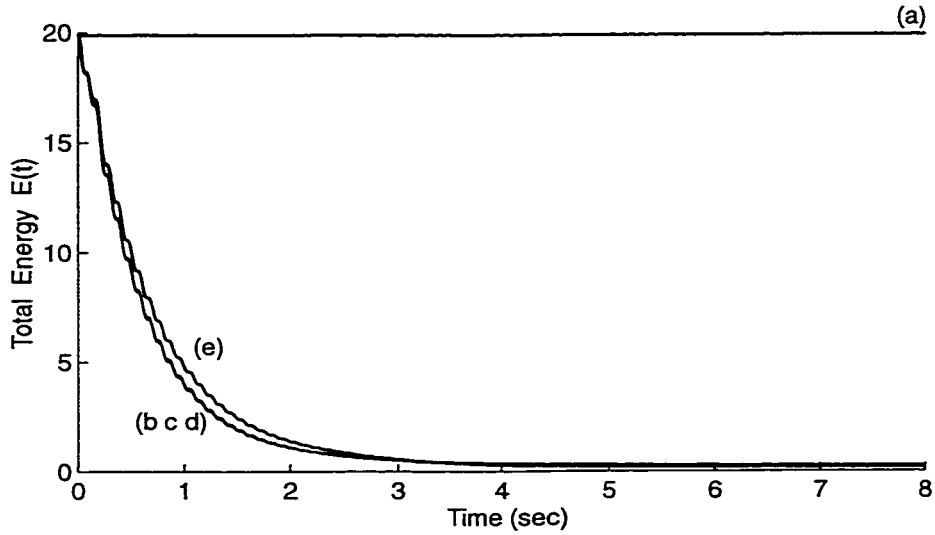

Figure 2.3 (a): Linear Case With Damping γ_1 & γ_{12}

	γ_1	γ_2	γ_{12}
a:	0	0	0
b:	10^{-4}	0	10^{-5}
c:	10^{-4}	0	10^{-4}
d:	10^{-4}	0	10^{-3}
e:	10^{-4}	0	10^{-2}

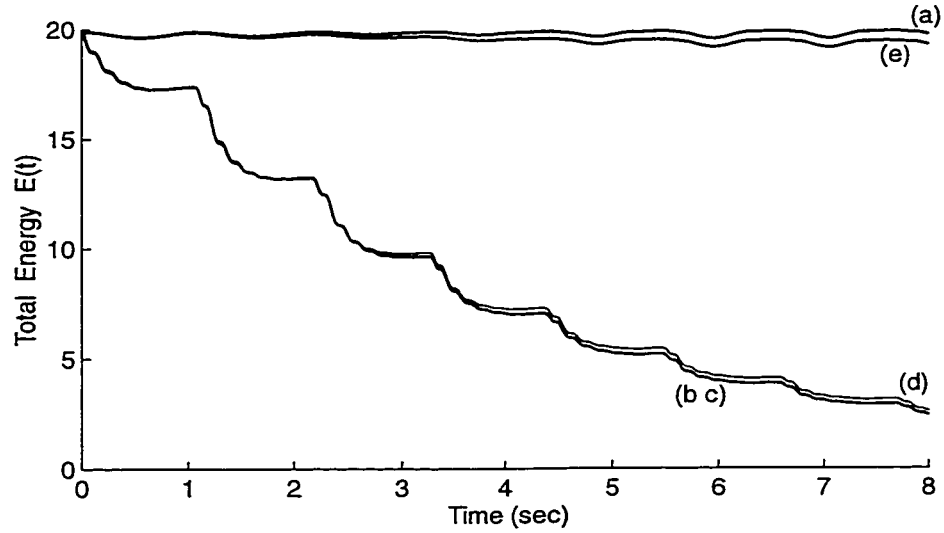

Figure 2.3 (b): Nonlinear Case With Damping γ_1 & γ_{12}

Chapter 3

Modelling of Torsional and Longitudinal Vibration of Suspension Bridge Subject to Aerodynamic Forces

3.1 General

This chapter considers a dynamic model of suspension bridge that is governed by a pair of coupled partial differential equations describing the torsional and longitudinal vibration of the road bed. The vertical and torsional motions are coupled through a nonlinear operation using the nonlinearity arising from loss of tension in the vertical cables supporting the deck. In addition, the impact of wind forces on the stability of motion of this system is studied both in the absence and presence of viscous and structural damping. Finaly, the results are illustrated through numerical simulation.

3.2 Model (B) (Torsional Motion):

A dynamic model of suspension bridge combining the aerodynamic forces caused by wind is presented as proposed by Roseau [14] as well as the nonlinear couplings due to loss of tension

in the vertical cables as suggested by Jacover and McKenna [13]. Thus, an approximate model that considers the torsional vibration of the road bed is given by the following system of partial differential equations:

$$\begin{cases} m\dfrac{\partial^2 z}{\partial t^2} + \beta_1 \dfrac{\partial^4 z}{\partial x^4} - \gamma_1 \dfrac{\partial^2 z}{\partial x^2} + KF_1(z,\theta) = f_1, \quad x \in (0,L), \quad t \geq 0, \\ \mathcal{I}\dfrac{\partial^2 \theta}{\partial t^2} + \beta_2 \dfrac{\partial^4 \theta}{\partial x^4} - \gamma_2 \dfrac{\partial^2 \theta}{\partial x^2} + K\ell F_2(z,\theta) = f_2, \quad x \in (0,L). \quad t \geq 0 \end{cases} \tag{3.1}$$

The suspension cable positions given by following equations:

$$\begin{cases} y_1 = \tilde{F}_0(z + \ell \ \sin\theta), \\ y_2 = \tilde{F}_0(z - \ell \ \sin\theta). \end{cases} \tag{3.2}$$

The two equations describe the displacement of the deck in the vertical plane from the rest position and the angle of twist of the road bed around the longitudinal axis from the horizontal plane respectively. This is known as torsional motion. In the equations, m is the mass per unit length of the bridge, $\mathcal{I} = 2m\ell^2$ is the mass moment of inertia (per unit length of the bridge) along the longitudinal axis, $\{\beta_1 = EI, \ \beta_2 = 2\ell^2\beta_1\}$ are the flexural rigidities, $\{\gamma_1 = (mg/8S)L^2, \ \gamma_2 = (KG + 2\ell^2\gamma_1)\}$ are the the coefficients of elasticity of the suspension cables and S is its sag.

The function $\tilde{F}_0(\xi)$ which signifies that if the vertical cables are loose, restraining force is zero and the suspension cables are free from the deck is given by:

$$\tilde{F}_0(\xi) = \begin{cases} \xi & \text{if } \xi < 0 \\ 0 & \text{otherwise} \end{cases} \tag{3.3}$$

The functions F_1 and F_2 are given by:

$$\begin{cases} F_1(z,\theta) \equiv \tilde{F}_0(z + \ell \ \sin\theta) + \tilde{F}_0(z - \ell \ \sin\theta), \\ F_2(z,\theta) \equiv (\tilde{F}_0(z + \ell \ \sin\theta) - \tilde{F}_0(z - \ell \ \sin\theta)) \cos\theta. \end{cases} \tag{3.4}$$

These functions consider the nonlinearity due to loss of tension in the vertical cables tied to the girders. The functions $\{f_1, f_2\}$ represent all nonconservative forces which include the aerodynamic forces.

3.2.1 Aerodynamic forces:

Using the analogy with Roseau's analysis [14, pp.236-239], the aeordynamic components of forces f_1 and f_2 can be given by:

$$\begin{cases} f_{1a} = 2\pi\rho\ell v^2 \left(\theta - \dfrac{1}{|v|}\left(\dfrac{\partial z}{\partial t}\right)\right), \\ f_{2a} = \pi\rho\ell^2 v^2 \left(\theta - \dfrac{1}{|v|}\left(\dfrac{\partial z}{\partial t}\right) - \dfrac{\ell}{|v|}\left(\dfrac{\partial \theta}{\partial t}\right)\right). \end{cases} \tag{3.5}$$

where ρ is the air density, v is the wind velocity with angle of attack ν with respect to the y-axis, and 2ℓ is the width of the bridge.

To solve the system of equations (3.1), the boundary and initial conditions for z and θ must be provided and are given in the following section.

3.3 Boundary and Initial Conditions

The decks are assumed clamped at both ends, giving the following boundary conditions

$$\begin{cases} z(t,0) = z(t,L) = 0, & \dfrac{\partial z}{\partial x}(t,0) = \dfrac{\partial z}{\partial x}(t,L) = 0 \\ \theta(t,0) = \theta(t,L) = 0, & \dfrac{\partial \theta}{\partial x}(t,0) = \dfrac{\partial \theta}{\partial x}(t,L) = 0. \end{cases} \tag{3.6}$$

In case the decks are hinged at both ends, the boundary conditions change to the following

$$\begin{cases} z(t,0) = z(t,L) = 0, & \dfrac{\partial^2 z}{\partial x^2}(t,0) = \dfrac{\partial^2 z}{\partial x^2}(t,L) = 0 \\ \theta(t,0) = \theta(t,L) = 0, & \dfrac{\partial^2 \theta}{\partial x^2}(t,0) = \dfrac{\partial^2 \theta}{\partial x^2}(t,L) = 0. \end{cases} \tag{3.7}$$

These boundary conditions must be valid at any time $t \geq 0$. In addition, the initial conditions are given by:

$$\begin{cases} z(0,x) = z_0(x), & \dfrac{\partial z}{\partial t}(0,x) = z_1(x) \\ \theta(0,x) = \theta_0(x), & \dfrac{\partial \theta}{\partial t}(0,x) = \theta_1(x). \end{cases} \tag{3.8}$$

$\{z_0,\ z_1,\ \theta_0,\ \theta_1\}$ are suitable functions which satisfy compatibily conditions with the boundary conditions considered.

3.4 Stability (Conservative System)

Lest's consider the system of equations (3.1),with (nonconservative forces), $f_1 = 0,\ \ f_2 = 0$, and the boundary conditions described by equations (3.6)-(3.7). The total energy functional is defined as a measure vibration of the bridge with respect to the body axes, considering all kinetic and potential energies of the system, is given by

$$
\begin{aligned}
E(t) \equiv\ & (1/2)\int_0^L \Big\{ \Big\{ m \left|\frac{\partial z}{\partial t}\right|^2 + \beta_1 \left|\frac{\partial^2 z}{\partial x^2}\right|^2 + \gamma_1 \left|\frac{\partial z}{\partial x}\right|^2 \Big\} \\
& + \Big\{ \mathcal{I} \left|\frac{\partial \theta}{\partial t}\right|^2 + \beta_2 \left|\frac{\partial^2 \theta}{\partial x^2}\right|^2 + \gamma_2 \left|\frac{\partial \theta}{\partial x}\right|^2 \Big\} \\
& + K\Big\{ G_0(z + \ell \sin\theta) + G_0(z - \ell \sin\theta) \Big\} \Big\} dx.
\end{aligned} \tag{3.9}
$$

with

$$
G_0(\eta) \equiv -\int_{-\eta}^{0} F_0(\xi) d\xi = -\int_0^{\eta} F_0(-\xi) d\xi.
$$

Using the boundary conditions (3.6)-(3.7) and the system equation (3.1), equation (3.10) can be verified as shown in section (2.5)

$$
\frac{dE(t)}{dt} \equiv 0, \quad t \geq 0. \tag{3.10}
$$

and hence the nonlinear system of equations (3.1) is also conservative.

In view of the above results, in absence of external forces a suspension bridge, linear or nonlinear, is conservative.

3.5 Asymptotic Stability (Damped System)

The external forces and torques f_1 and f_2 can be written as

$$
\begin{cases}
f_1 \equiv f_{1a} + f_{1v} + f_{1s} \\
f_2 \equiv f_{2a} + f_{2v} + f_{2s}
\end{cases} \tag{3.11}
$$

where $f_{i,a}$, $f_{i,v}$, $f_{i,s}$ $i = 1, 2$ represent the aerodynamic forces, the viscous forces and the forces exerted by the structural elastic resistance,respectively. For wind velocity $v = 0$, the

forces f_{1a} and f_{2a} are equal to zero.Therefore, when only viscous and structural dampings are present, we have the following:

$$\begin{cases} f_1 = f_{1v} + f_{1s} \equiv -k_{11}\left(\dfrac{\partial z}{\partial t}\right) + k_{12}\left(\dfrac{\partial^2}{\partial x^2}\left(\dfrac{\partial z}{\partial t}\right)\right) - k_{13}\left(\dfrac{\partial^4}{\partial x^4}\left(\dfrac{\partial z}{\partial t}\right)\right) \\ f_2 = f_{2v} + f_{2s} \equiv -k_{21}\left(\dfrac{\partial \theta}{\partial t}\right) + k_{22}\left(\dfrac{\partial^2}{\partial x^2}\left(\dfrac{\partial \theta}{\partial t}\right)\right) - k_{23}\left(\dfrac{\partial^4}{\partial x^4}\left(\dfrac{\partial \theta}{\partial t}\right)\right), \end{cases} \tag{3.12}$$

Here we are interested in stability as the question of existence and regularity properties of solutions are studied in [21]. Taking the first derivative with respect to time of equation (3.9) and using the system of equations (3.1) and the boundary conditions (3.6)-(3.7) we obtain

$$\begin{aligned} \frac{dE(t)}{dt} &= \int_0^L \left\{ f_1\left(\frac{\partial z}{\partial t}\right)\frac{\partial z}{\partial t} + f_2\left(\frac{\partial \theta}{\partial t}\right)\frac{\partial \theta}{\partial t} \right\} dx \\ &= -\int_0^L \left\{ \left\{ k_{11}\left|\frac{\partial z}{\partial t}\right|^2 + k_{12}\left|\frac{\partial}{\partial x}\left(\frac{\partial z}{\partial t}\right)\right|^2 + k_{13}\left|\frac{\partial^2}{\partial x^2}\left(\frac{\partial z}{\partial t}\right)\right|^2 \right\} \right. \\ &+ \left. \left\{ k_{21}\left|\frac{\partial \theta}{\partial t}\right|^2 + k_{22}\left|\frac{\partial}{\partial x}\left(\frac{\partial \theta}{\partial t}\right)\right|^2 + k_{23}\left|\frac{\partial^2}{\partial x^2}\left(\frac{\partial \theta}{\partial t}\right)\right|^2 \right\} \right\} dx \le 0. \end{aligned} \tag{3.13}$$

Using equations (3.1) and (3.13) along with the boundary conditions (3.6)-(3.7), it ca be shown that $\dfrac{dE(t)}{dt} < 0$, for all $t > 0$, as well as that the system is asymptotically stable. The following result can be obtained.

Theorem 3.2

Consider the system (3.1) and (3.6)-(3.7) and suppose the forces $\{f_1\ ,\ f_2\}$ are as given by (3.12). Then the system is asymptotically stable if any one of the pairs $\{(k_{1i},\ k_{2j}),\ i,j = 1,2,3\}$ is strictly positive.

Remark.

Another proof is given by use of semigroup theory (see Abstract Model in [21]).

3.6 Numerical Results and Discussions

The stability properties of the suspension bridge described by (3.1)-(3.6), can be investigated through a numerical simulation.

The data used in the simulation are listed as follows:

$$m = 10,\quad \beta_1 = 10,\quad \gamma_1 = 0.035,\quad K = 10,\quad \rho = 1.18,\quad L = 1,\quad \ell = 0.05,$$

$$\mathcal{I} = 2m\ell^2 = 0.05,\quad \beta_2 = 2\ell^2\beta_1 = 0.05,\quad G = 0.18,\quad \gamma_2 = (KG + 2\ell^2\gamma_1) = 1.8.$$

To ensure numercal stability, the ratio $(\Delta t/\Delta x) = 2 \times 10^{-3}$ was chosen.

The aerodynamic forces as given by equation (3.5) are as follows:

$$\begin{cases} f_{1a} = 2\pi\rho\ell v^2\left(\theta - \dfrac{1}{|v|}\left(\dfrac{\partial z}{\partial t}\right)\right), \\ \\ f_{2a} = \pi\rho\ell^2 v^2\left(\theta - \dfrac{1}{|v|}\left(\dfrac{\partial z}{\partial t}\right) - \dfrac{\ell}{|v|}\left(\dfrac{\partial\theta}{\partial t}\right)\right), \end{cases}$$

These equations provide viscous damping through the second term in the first equation, and second and third terms in the second equation. The destabilizing effect is shown by other two terms. For this simulation, two sets of graphs are presented. For the first set, the normal viscous damping is assumed to be negligible, except for the damping components arising from the wind activities as mentioned above. Figures 3.1 - 3.4 give the results on total energy and vertical and torsional displacements as a function of increasing mean wind velocity v. These figures clearly show that even though initially $\theta(0,x) = \theta_t(0,x) \equiv 0$, the vertical motion induces torsional motion (see Figures 3.2(c), 3.3(c) and 3.4(c). Further,

at low wind velocities, the aerodynamic damping components are predominant which leads to decay of initial energy (see Figures 3.1(a), 3.2(a) and 3.3(a)). Furthermore, with more increase of wind velocity (see Figure 3.4(a)) the destabilizing factors, dominate over the aerodynamic damping forces and lead to high and consequently catastrophic increase of energy. The second set of results are similar to those of the first set for naturally damped system, i.e., it is assumed that the normal viscous damping component provided by the surrouding atmosphere (at normal temperature and pressure) at zero wind velocity is not negligible. The results are dipicted in Figures 3.5 - 3.9. Comparing the energy plots of Figures 3.1(a), 3.2(a), 3.3(a) and 3.4(a) with those of Figures 3.5(a), 3.6(a), 3.7(a) and 3.8(a), it can be concluded that the presence of small natural damping has some stabilizing effect up to a larger wind velocity. For the undamped system (Figure 3.4(a)), the oscillations experienced by the bridge are catastrophic at $\nu = 50$ while for the naturally damped system (Figure 3.8(a)), at the same wind velocity, the bridge experiences oscillation but not so catastrophic. However, for $\nu = 60$ catastrophic oscillation sets in as shown in Figure 3.9.

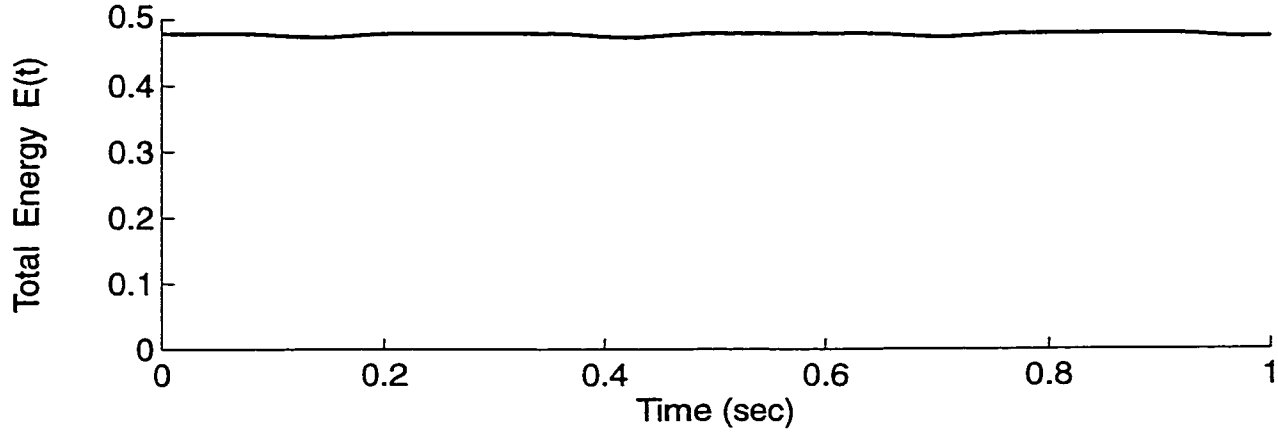

(a)

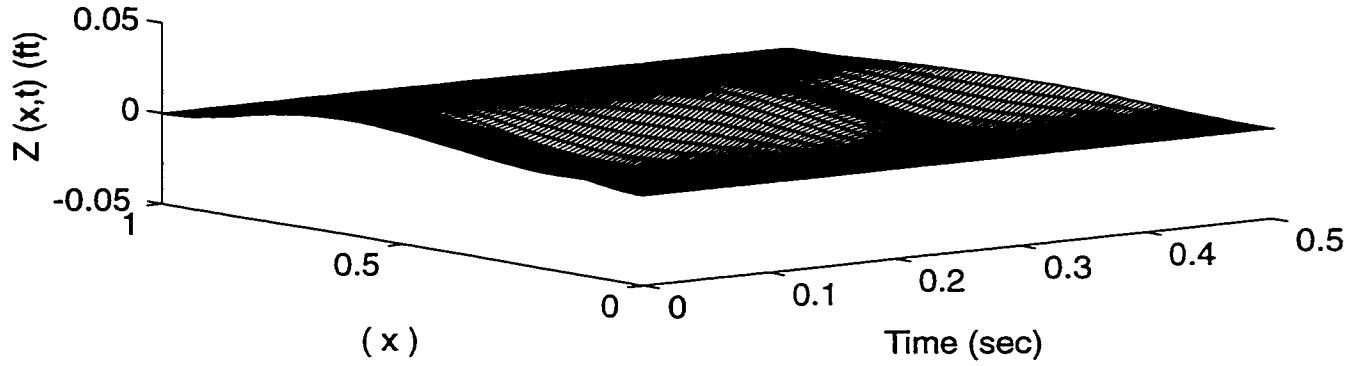

(b)

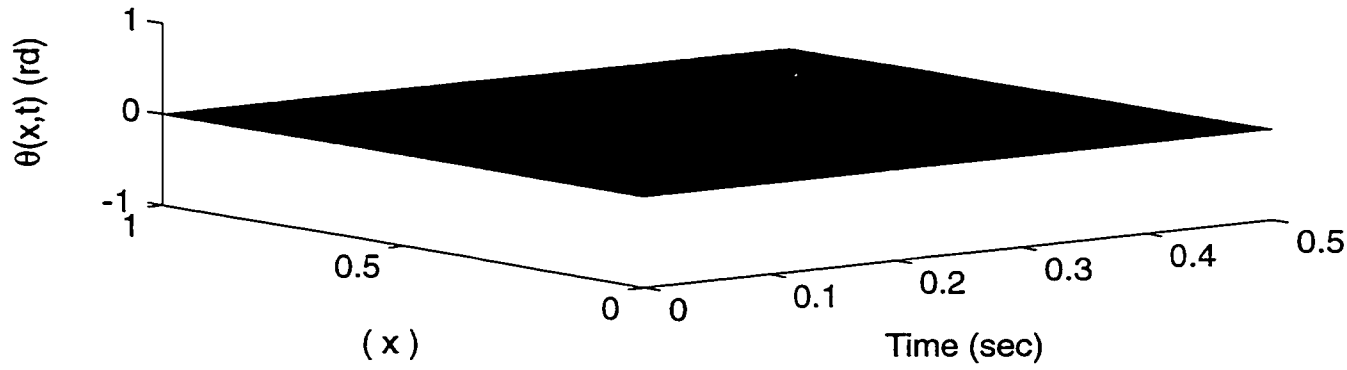

(c)

FIGURE 3.1 Undamped system, $V = 0$ m/s

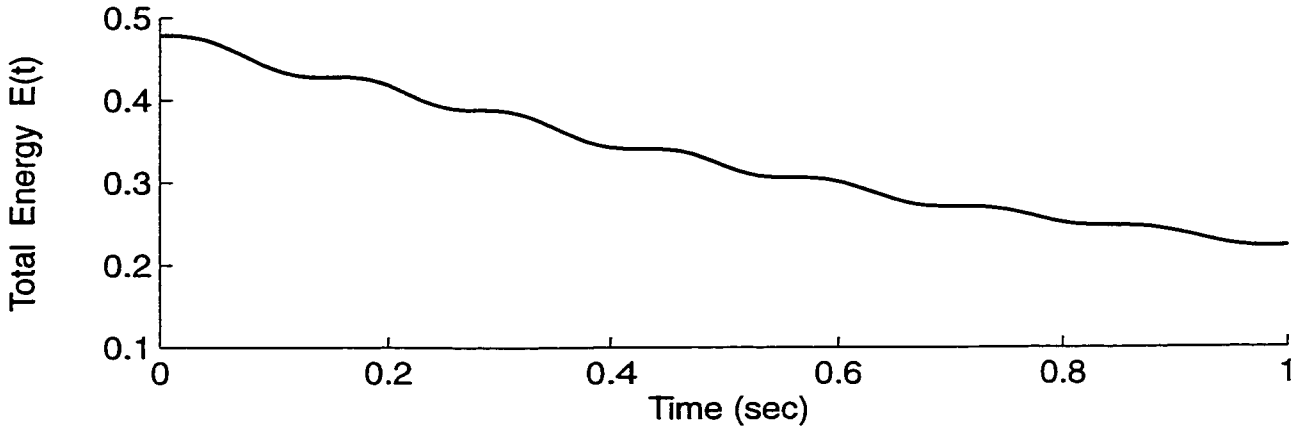

(a)

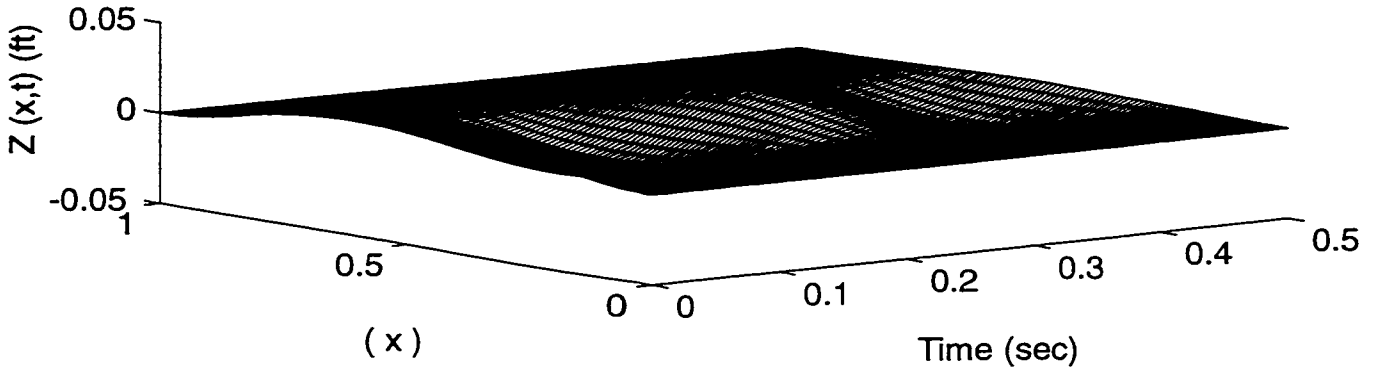

(b)

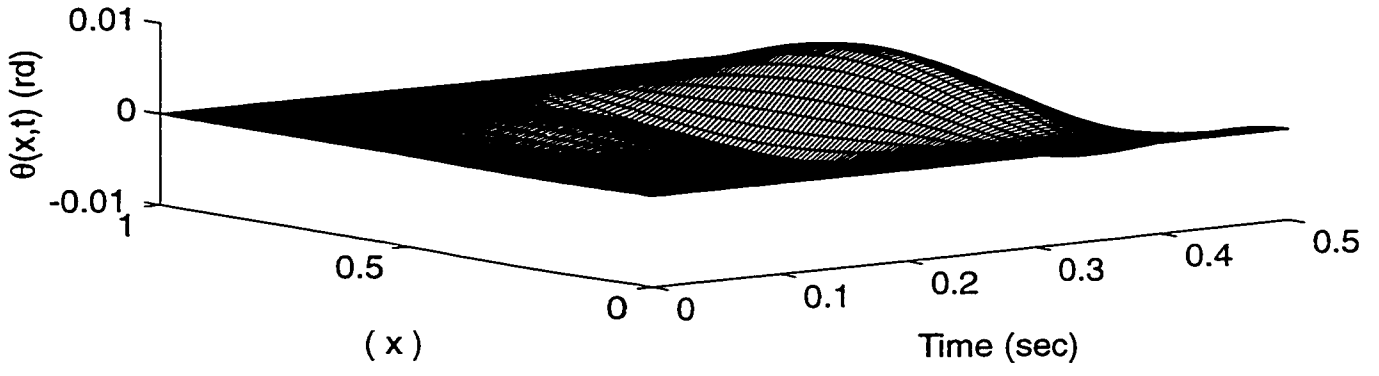

(c)

FIGURE 3.2 Undamped system, $V = 18$ m/s

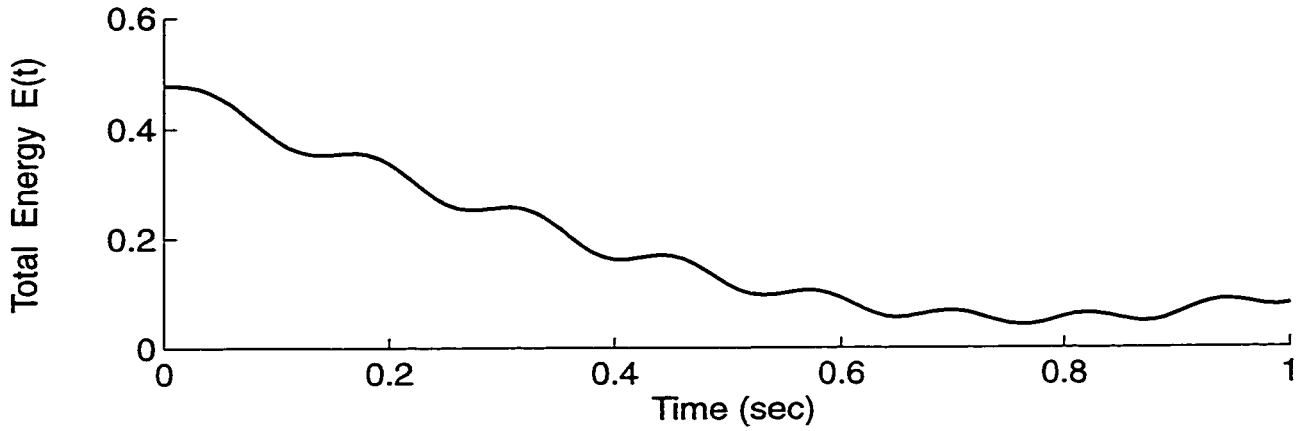

(a)

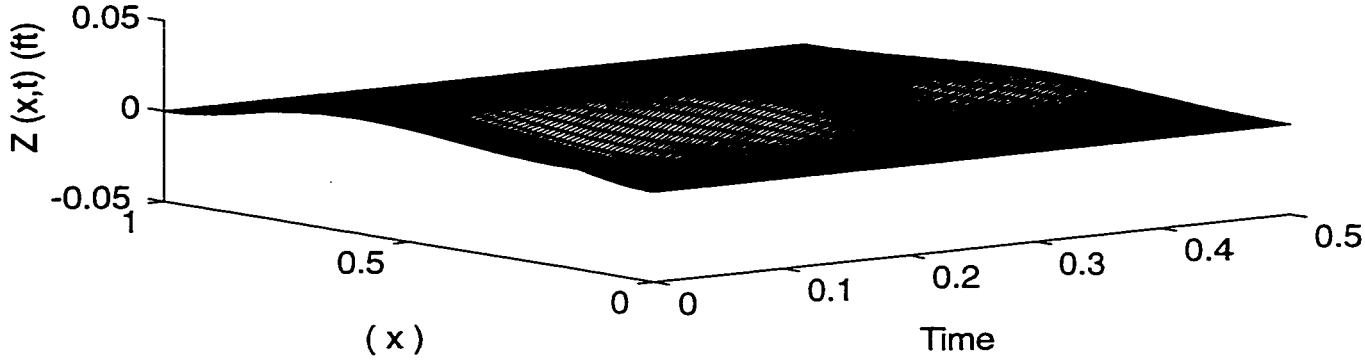

(b)

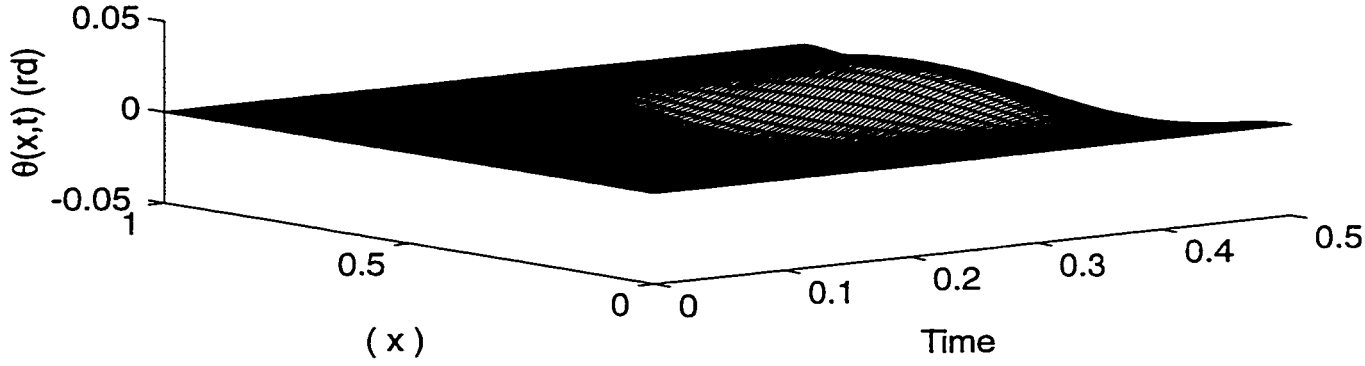

(c)

FIGURE 3.3 Undamped system, $V = 40$ m/s

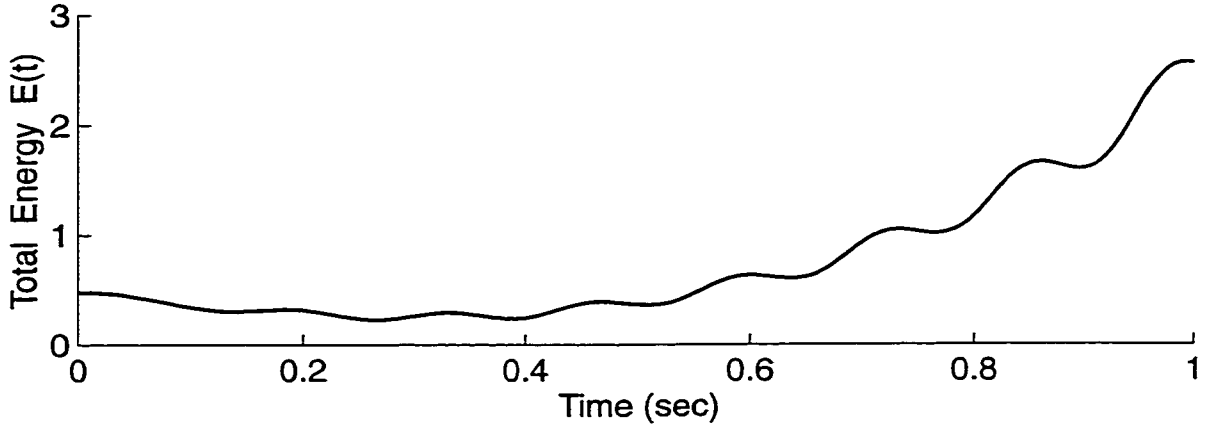

(a)

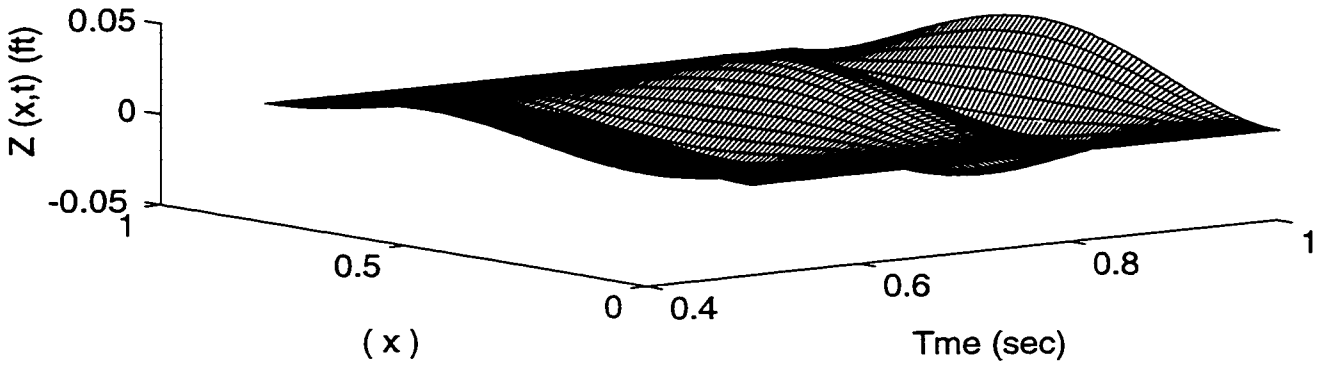

(b)

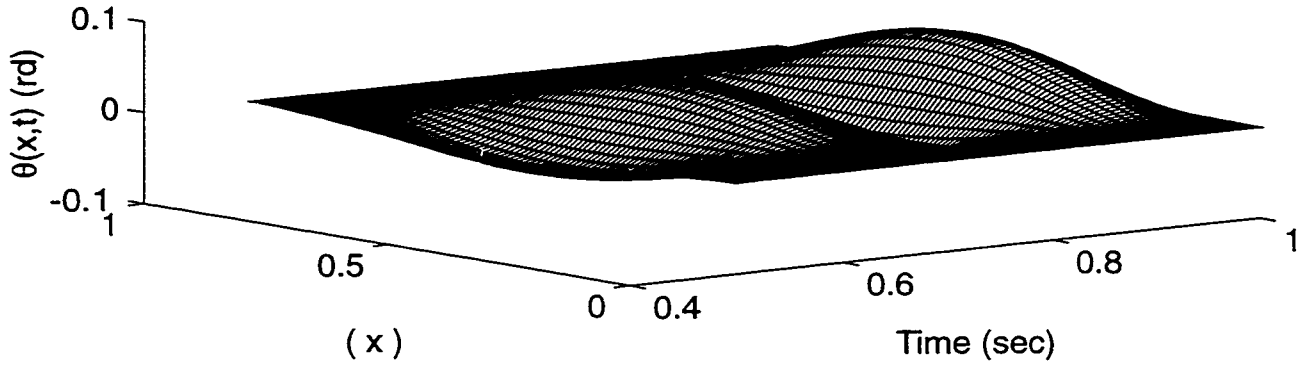

(c)

FIGURE 3.4 Undamped system, $V = 50$ m/s

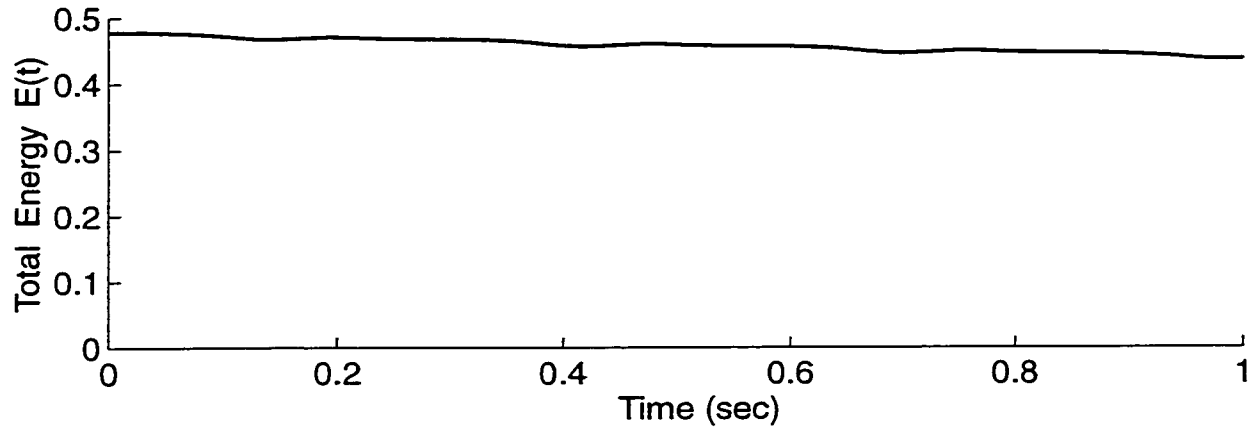

(a)

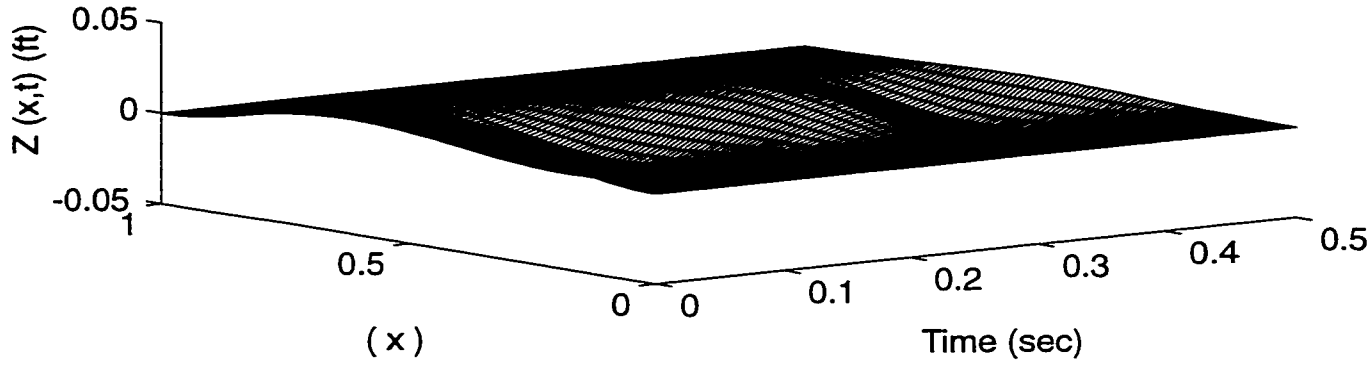

(b)

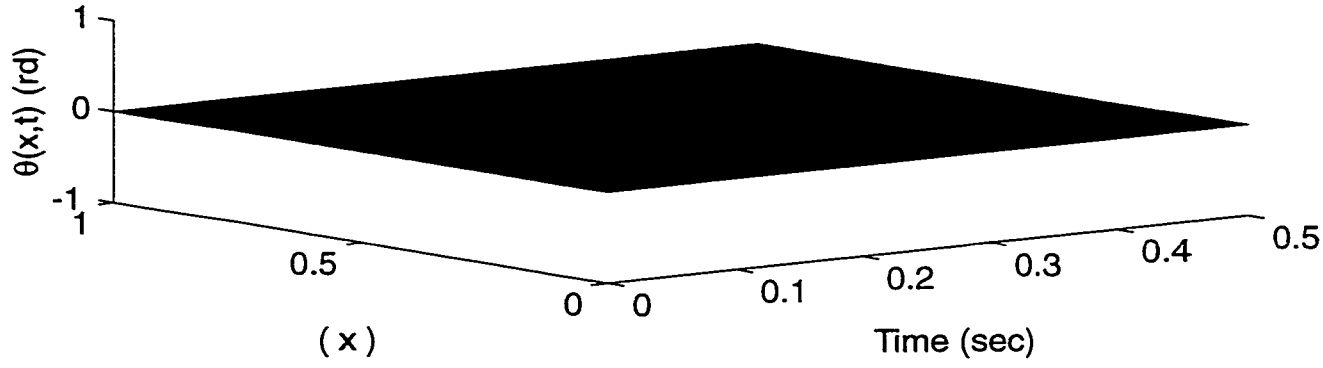

(c)

FIGURE 3.5 Damped system, $V = 0$ m/s

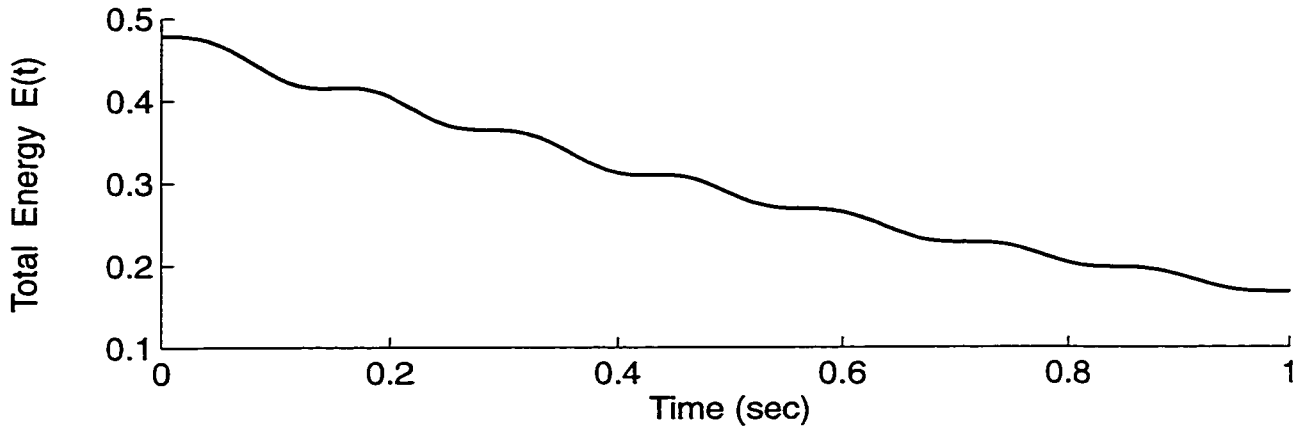

(a)

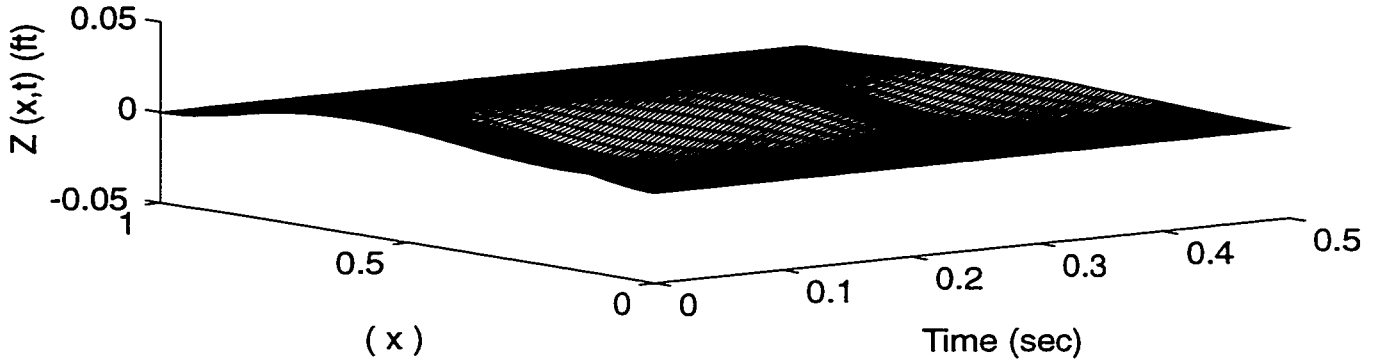

(b)

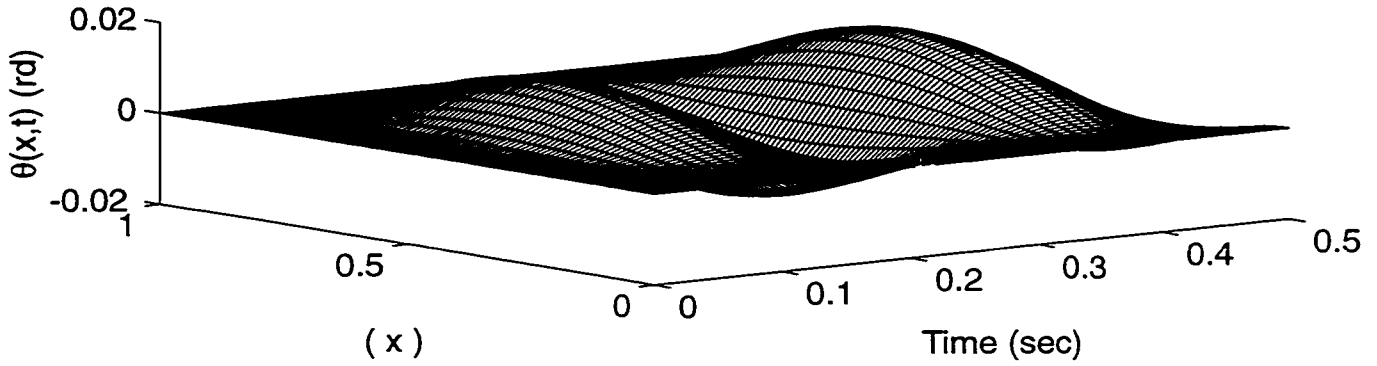

(c)

FIGURE 3.6 Damped system, $V = 18$ m/s

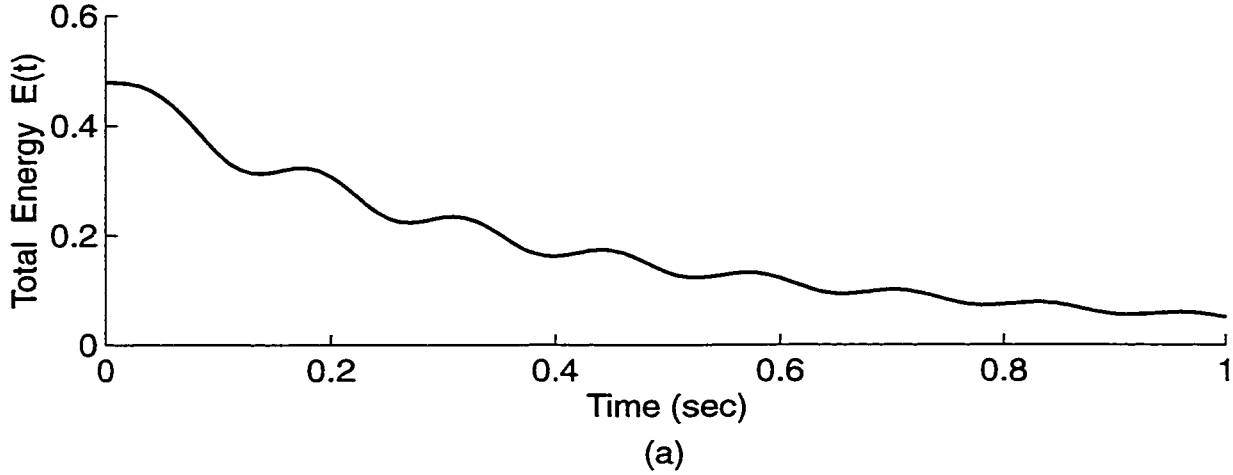

(a)

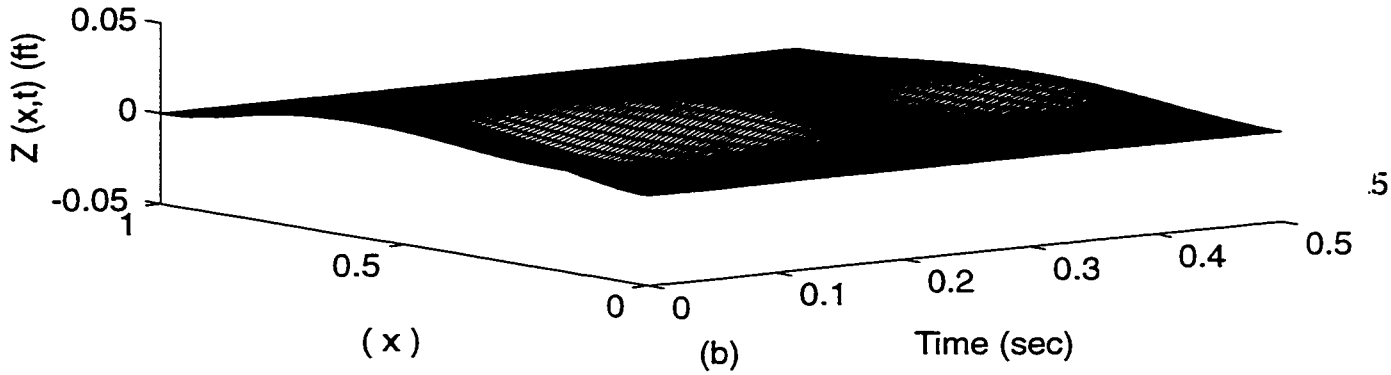

(b)

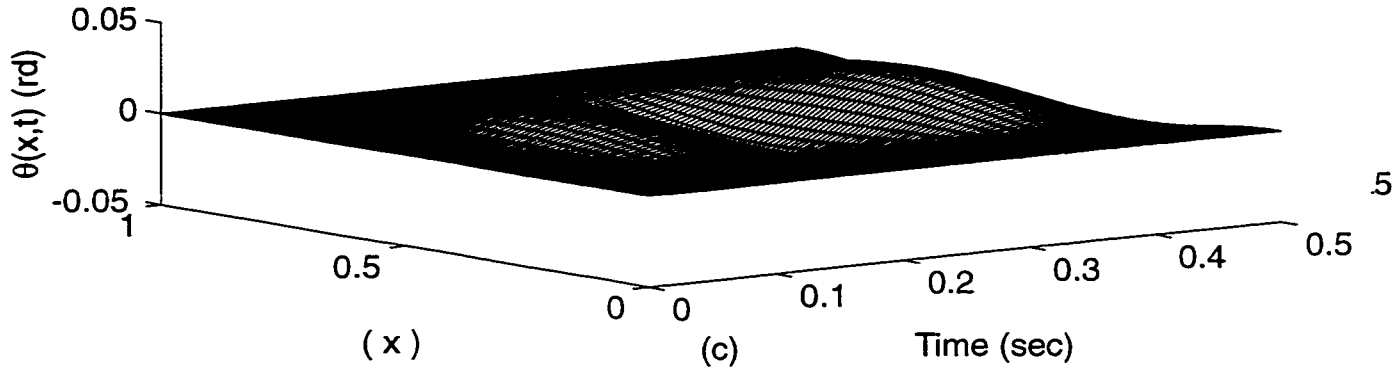

(c)

FIGURE 3.7 Damped system, $V = 40$ m/s

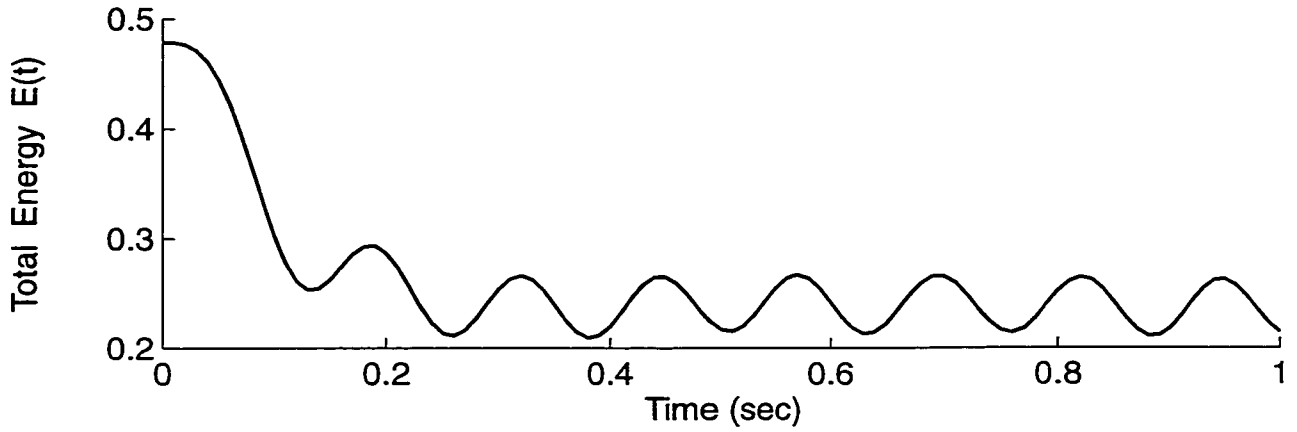

(a)

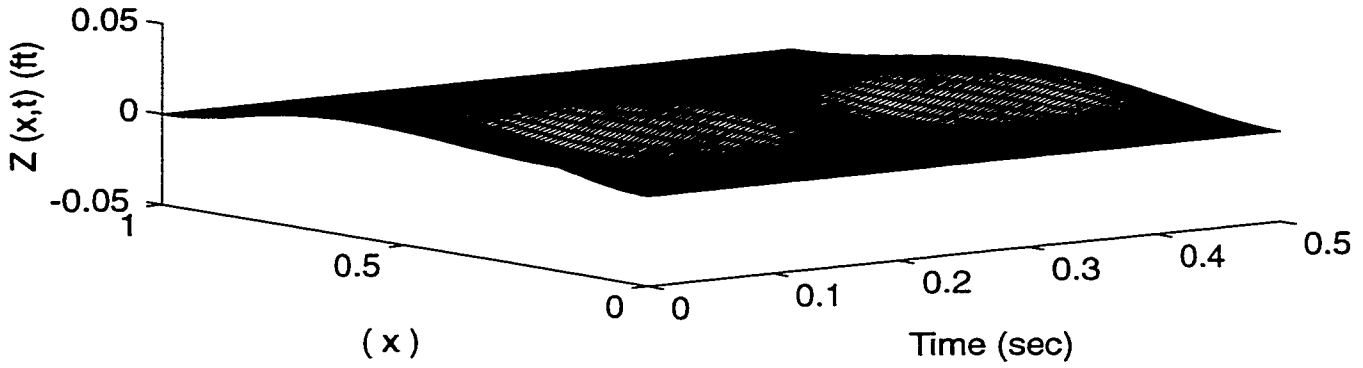

(b)

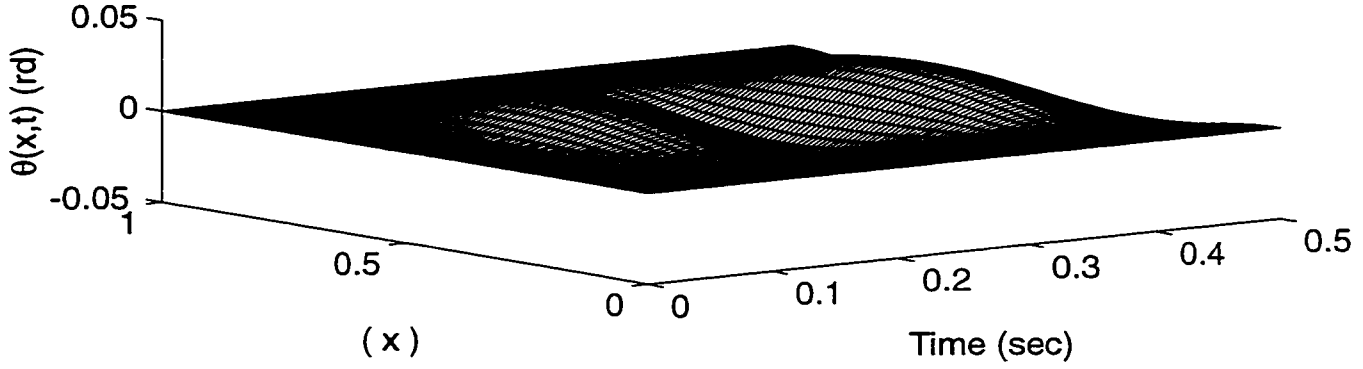

(c)

FIGURE 3.8 Damped system, $v = 50$ m/s

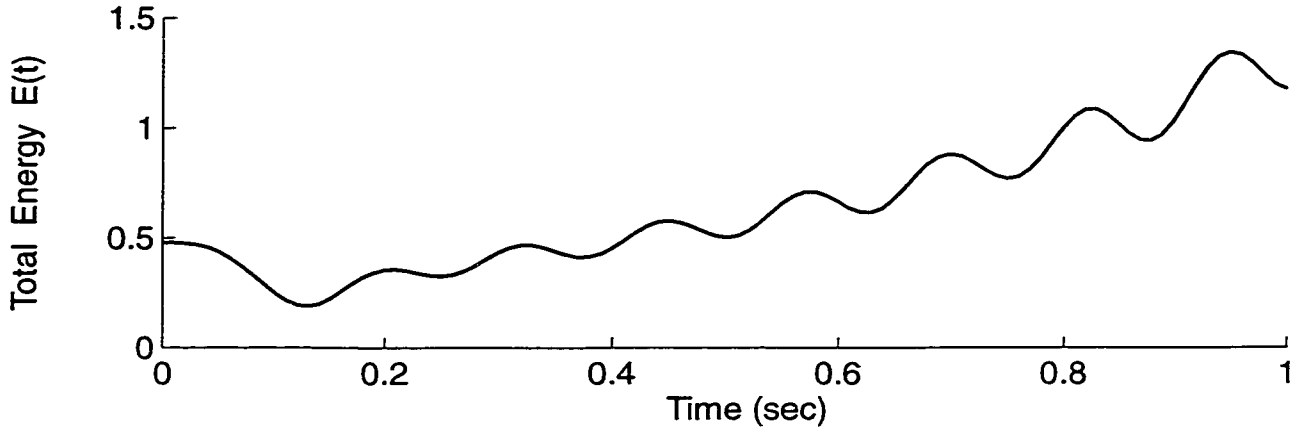

(a)

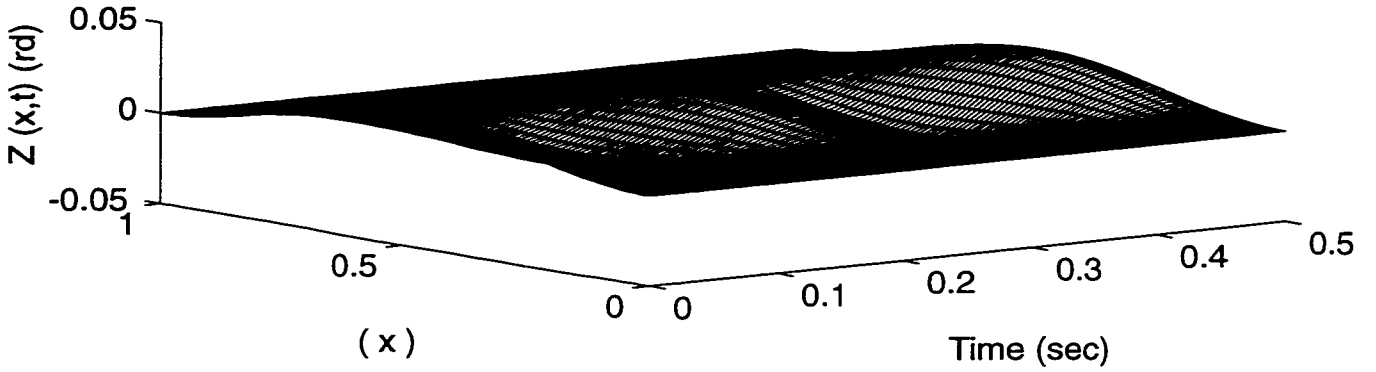

(b)

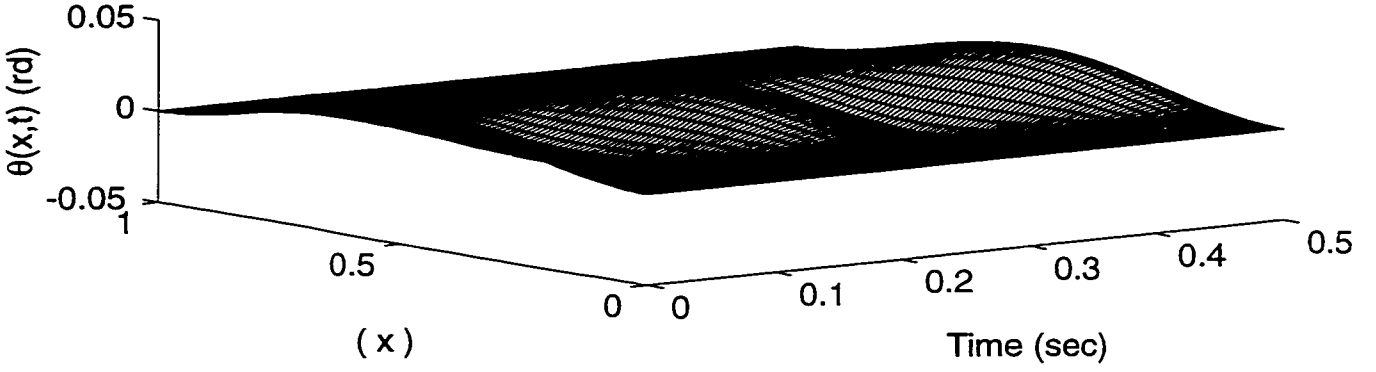

(c)

FIGURE 3.9 Damped system, $V = 60$ m/s

Chapter 4

Stochastic Modelling and Stability of Suspension Bridge

4.1 General

A suspension bridge is often subjected to random disturbances arising from various sources such as wind and seismic activities as well as normal vehicular load. These disturbances may produce random torques and random spatially distributed forces on the structure which may destabilize the system. This study considers only wind forces. Chapter 3 studied the impact of deterministic wind forces on the structure, which was based on fundamental analysis developed in [16]. In [32], a general mathematical frame work was established for analysis of suspension bridges subject to random forces without any numerical results. In this chapter, the deterministic results of [21] are extended to stochastic case and several simulation results are presented. A well designed suspension bridge can sustain a certain level of vertical and torsional motions without reaching unstablility. If disturbances persist, even small motions under moderate wind forces may build up and lead to instability of the system. In this chapter, the wind forces are modeled as a random process and the impact of such forces on the stability of motion of the system is studied. Finally, the results are illustrated by some numerical examples.

4.2 System Model

To model the system, the concepts of Roseau [14], Ahmed and Harbi [16], Lazer and McKenna [10] and Jacover and McKenna [13] are used. Combining these concepts, an approximate model that includes both vertical and torsional motions of the road bed is developed and given by:

$$\begin{cases} m\dfrac{\partial^2 z}{\partial t^2} + \beta_1\dfrac{\partial^4 z}{\partial x^4} - \gamma_1\dfrac{\partial^2 z}{\partial x^2} + KF_1(z,\theta) = f_1, \quad x \in (0,L), \quad t \geq o. \\ \mathcal{I}\dfrac{\partial^2 \theta}{\partial t^2} + \beta_2\dfrac{\partial^4 \theta}{\partial x^4} - \gamma_2\dfrac{\partial^2 \theta}{\partial x^2} + K\ell F_2(z,\theta) = f_2, \quad x \in (0,L), \quad t \geq 0, \end{cases} \tag{4.1}$$

f_1 and f_2 denote all the external (non conservative) forces acting on the system. In case of vertical lift, the suspension cables may loose tension and consequently the system behaves nonlinearly. The functions F_1 and F_2 denote the restraining forces which depend on vertical displacement and tilt of the panel providing also the nonlinear coupling between the two modes of motion.

The vertical positions of the two suspension cables are given by the following

$$\begin{cases} y_1 = \tilde{F}_0(z + \ell\sin\theta), \\ y_2 = \tilde{F}_0(z - \ell\sin\theta). \end{cases} \tag{4.2}$$

In the system (4.1), the first equation describes the vibration of the road bed in the vertical plane and the second equation describes its torsional motion.

The parameters appearing in the above equations have the following physical interpretations: m = the mass per unit length of the bridge , 2ℓ = the width of the deck, $\mathcal{I} = 2m\ell^2$ = the mass moment of inertia per unit length of the bridge, $\beta_1 = EI$ and $\beta_2 = 2\ell^2\beta_1$ are the

flexural rigidities the flexural rigidity, $\gamma_1 = (mg/8S)L^2$ = tensile stress, $\gamma_2 = (kG + 2\ell^2\gamma_1)$ = torsional stress S = sag of the suspension cables . The function $\tilde{F}_0$ which represents the normalized restraining force signifying that if the vertical cables are loose, restraining force is zero and the suspension cables are free from the deck is defined as follows:

$$\tilde{F}_0(\xi) = \begin{cases} \xi & \text{if } \xi < 0 \\ \\ 0 & \text{otherwise.} \end{cases} \tag{4.3}$$

Considering a tilted panel with tilt angle θ (with respect to horizontal plane) and vertical displacement z (of the center line of the panel). and using plain geometry it can be verified that the functions F_1 and F_2 are given by

$$\begin{cases} F_1(z,\theta) \equiv \tilde{F}_0(z + \ell\sin\theta) + \tilde{F}_0(z - \ell\sin\theta). \\ \\ F_2(z,\theta) \equiv \left(\tilde{F}_0(z + \ell\sin\theta) - \tilde{F}_0(z - \ell\sin\theta)\right)\cos\theta. \end{cases} \tag{4.4}$$

These functions take into account the restraining forces and the nonlinear coupling that arises due to loss of tension in the vertical cables tied to the girders. The functions $\{f_1\ ,\ f_2\}$ represent all nonconservative and external forces such as aerodynamic forces.

Using Roseau's analysis [14], the aerodynamic components of the forces f_1 and f_2 are given by:

$$\begin{cases} f_{1a} = 2\pi\rho\ell v^2\left((\theta - \nu) - \dfrac{1}{|v|}\left(\dfrac{\partial z}{\partial t}\right)\right), \\ \\ f_{2a} = \pi\rho\ell^2 v^2\left((\theta - \nu) - \dfrac{1}{|v|}\left(\dfrac{\partial z}{\partial t}\right) - \dfrac{\ell}{|v|}\left(\dfrac{\partial\theta}{\partial t}\right)\right), \end{cases} \tag{4.5}$$

where ρ = the air density, v = the wind velocity, ν = the angle of attack with respect to the horoizontal plane.

In order to solve the system of equations (4.1), boundary and initial conditions for z and θ must be specified. Assuming that the middle section is clamped to the bays at both ends, the boundary conditions can be written as shown below:

$$\begin{cases} z(t,0) = z(t,L) = 0, & \dfrac{\partial z}{\partial x}(t,0) = \dfrac{\partial z}{\partial x}(t,L) = 0 \\ \theta(t,0) = \theta(t,L) = 0, & \dfrac{\partial \theta}{\partial x}(t,0) = \dfrac{\partial \theta}{\partial x}(t,L) = 0. \end{cases} \tag{4.6}$$

For hinged end conditions, the boundary are given by:

$$\begin{cases} z(t,0) = z(t,L) = 0, & \dfrac{\partial^2 z}{\partial x^2}(t,0) = \dfrac{\partial^2 z}{\partial x^2}(t,L) = 0 \\ \theta(t,0) = \theta(t,L), & \dfrac{\partial^2 \theta}{\partial x^2}(t,0) = \dfrac{\partial^2 \theta}{\partial x^2}(t,L) = 0. \end{cases} \tag{4.7}$$

These boundary conditions must hold for all $t \geq 0$. The initial conditions are given by

$$\begin{cases} z(0,x) = z_0(x), & \dfrac{\partial z}{\partial t}(0,x) = z_1(x) \\ \theta(0,x) = \theta_0(x), & \dfrac{\partial \theta}{\partial t}(0,x) = \theta_1(x), \end{cases} \tag{4.8}$$

with $\{z_0, z_1, \theta_0, \theta_1\}$ suitable functions satisfying conditions compatible with the specified boundary conditions.

4.3 Stochastic Model of Aerodynamic forces

The aerodynamic forces acting on the bridge are not fully deterministic because of gusty ness of the wind blowing past the structure. The wind velocity is modeled as a random process which may be distributed in space and time. Except for a too large bridge span, it may be

assumed that the wind activities be spatially uniform surrounding the region occupied by the bridge. For stochastic analysis, the wind velocity is given by a sum of two components $v = v_0 + \hat{v}$ where v_0 denotes the normal wind velocity in the region and $\hat{v}$ its fluctuation. The random fluctuation is modeled by a stochastic differential equation,

$$d\hat{v} = a(t)dt + \sigma(t)dw_\alpha(t), \hat{v}(0) = 0 \tag{4.9}$$

where $a(t)$ denotes the mean acceleration and $\sigma(t)$ denotes the volatility or gusty nature of the wind and w_α denotes the time scaled (by the factor $\alpha >> 1$) one dimensional standard Brownian motion. Since the movement of mechanical structures are significantly slower compared to that of standard Brownian motion, it is necessary to scale it down so that it is comparable or compatible with the motion of mechanical structures. In view of the expression (4.5) and equation (4.9), the aerodynamic forces are now random and they are given by:

$$\begin{cases} \hat{f}_{1\alpha} = 2\pi\rho\ell v^2 \left((\theta - \nu) - \dfrac{1}{|v|} \left(\dfrac{\partial z}{\partial t} \right) \right), \\ \hat{f}_{2\alpha} = \pi\rho\ell^2 v^2 \left((\theta - \nu) - \dfrac{1}{|v|} \left(\dfrac{\partial z}{\partial t} \right) - \dfrac{\ell}{|v|} \left(\dfrac{\partial \theta}{\partial t} \right) \right). \end{cases} \tag{4.10}$$

where

$$v(t) = v_0 + \int_0^t a(s)ds + \int_0^t \sigma(s)dw_\alpha \tag{4.11}$$

The angle of attack ν can also be a random process or simply a random variable. In some of our numerical simulation experiments, used two different processes for angle of attack were used such as $\nu(t) = \zeta \sin \Delta w_\alpha(t)$ and $\nu(t) = \zeta \ sign \ [\sin \Delta w_\alpha(t)]$, where $\zeta \in (-\pi/2, +\pi/2)$. The increments can be replaced by the Brownian motion itself.

4.4 Response to Stochastic Load

The impact of wind forces on the stability of motion of suspension bridges was studied in chapter 3. This is extended to the stochastic case in this chapter.

For a Lyapunov function we may choose the energy function $E(t)$ given by

$$\begin{aligned} E(t) &\equiv (1/2)\int_0^L \{[m(z_t)^2 + \beta_1(D^2 z)^2 + \gamma_1(Dz)^2] + [\mathcal{I}(\theta_t)^2 + \beta_2(D^2\theta)^2 + \gamma_2(D\theta)^2\} \\ &+ 2K[G_0(z + \ell\ sin\ \theta) + G_0(z - \ell\ sin\ \theta)]\}dx, \end{aligned} \tag{4.12}$$

where the first six terms represent the sum of kinetic and potential energies of the deck considering both the vertical and torsional motions. The last two terms denote the elastic potential energy of the (vertical) cables attached to the girders. The function G_0 is given by:

$$G_0(\eta) = -\int_0^\eta F_0(-\xi)d\xi. \tag{4.13}$$

In the absence of external forces, ($f_1 = f_2 = 0$), the system (4.1) can be shown to be conservative. Indeed, by taking the time first derivative of this energy functional and integrating by parts and using the system equation (4.1) along with the boundary conditions (4.6), it can be verified that $\frac{dE(t)}{dt} \equiv 0$. Therefore, in the absence of external forces, the system is conservative. This is because the viscous damping and friction are assumed to be negligible, although there is always some viscous damping and friction for a mechanical structure like a bridge. The friction is caused by relative motion of the parts that constitute the whole structure.

Our objective now is to compute the energy functional while the system is subject to stochastic wind load. We shall compute the energy functional for different angles of attacks, ν, as a parameter. For comparison, we shall do the same assuming that the system possesses some internal or structural damping. The internal damping can be improved by use of smart

materials such as piezo ceramic layers used in the construction of the girders and panels of the deck.

4.5 Numerical Results and Discussions

In this section, simulation results and discussions are presented. The basic parameters for the simulations are:

$$L = 1, 2\ell = 0.1, m = 10, I = 0.05, \beta_1 = 10, \beta_2 = 0.05,$$

$$\gamma_1 = 0.035, \gamma_2 = 1.8, K = 10, \rho = 1.8, v_0 = 18.$$

The finite difference method with FORTRAN Language was used to solve the equations. For numerical stability the ratio $(\triangle t/\triangle x)$ was chosen as 2×10^{-3}. For simulation experiment, Gaussian noise process was generated using MATLAB Software on SUN SPARC Station 5 and numerical integration was carried out using a Runge-Kutta - like algorithm as discussed in [31]. To create a gusty wind environment, the functions a and σ of equation (4.9) were chosen as follows:

$$\begin{cases} a(t) = k\phi(t)\sin 2\pi t \\ \\ \sigma(t) = \gamma\phi(t) \end{cases} \tag{4.14}$$

where

$$\phi(t) = \begin{cases} 1 & \text{if } t \in [0, 1] \\ \\ 0 & \text{otherwise} \end{cases} \tag{4.15}$$

This represents start of severe wind conditions at time time $t = 0$ and it ends at time $t = 1$ attaining maximum velocity at $t = (1/2)$. In equation (4.14), k denotes peak intensity of the wind acceleration and γ^2 is a measure of its fluctuation energy.

The response of the bridge, in the absence of damping (viscous or and structural), is shown in the graphs Figures 4.1 - 4.3. As shown in Figure 4.1(a), the wind velocity is plotted as

a function of time. The corresponding response of the structure is shown in Figures 4.1(b), 4.2(a), 4.2(b), 4.3(a), 4.3(b), 4.3(c). The total system energy, as given by the expression (4.12), is illustrated in Figure 4.1(b) for different angles of attack ($\nu = 40^o, 30^o, 20^o$.) The corresponding vertical and torsional motions are displayed in Figure 4.2(a) and Figur 4.2(b). It is clear from the results that the system is unstable. Similar results are also displayed in the Figures 4.3(a), 4.3(b), 4.3(c) for angles of attack ($\nu = 10^o, 0^o$). Only in case of $\nu = 0$, the system remains stable.

Next we assume that the panels are coated with smart materials providing structural damping. We expect that the dissipative forces produced by material damping have the general form

$$f = f(D^2 z_t, D^4 z_t).$$

In the linear case, the forces f_{1d} (and torques f_{2d}) are given by

$$\begin{cases} f_{1d} = \delta_1 D^2 z_t - \tilde{\delta}_1 D^4 z_t \\ f_{2d} = \delta_2 D^2 \theta_t - \tilde{\delta}_2 (D^4 \theta_t), \end{cases} \tag{4.16}$$

where $\delta_1, \tilde{\delta}_1, \delta_2, \tilde{\delta}_2$ are nonnegative constants which may be different for different materials. Thus the total external and nonconservative forces acting on the system (4.1) are given by

$$\begin{cases} f_1 = f_{1a} + f_{1d} \\ f_2 = f_{2a} + f_{2d}. \end{cases} \tag{4.17}$$

For numerical simulation, $\delta_1 = \delta_2 = 0.8$ is assumed and the higher order dampings are neglected. The wind conditions are assumed to be the same as that of the undamped case. The corresponding results are plotted in Figures 4.4(a, 4.4(b), 4.5(a), 4.5(b), 4.6(a), 4.6(b), 4.6(c). The results show that the system is now asymptotically stable. Both vertical and

torsional motions asymptotically decay to zero after the storm has passed. Thus the presence of structural damping provides a powerful dissipation mechanism.

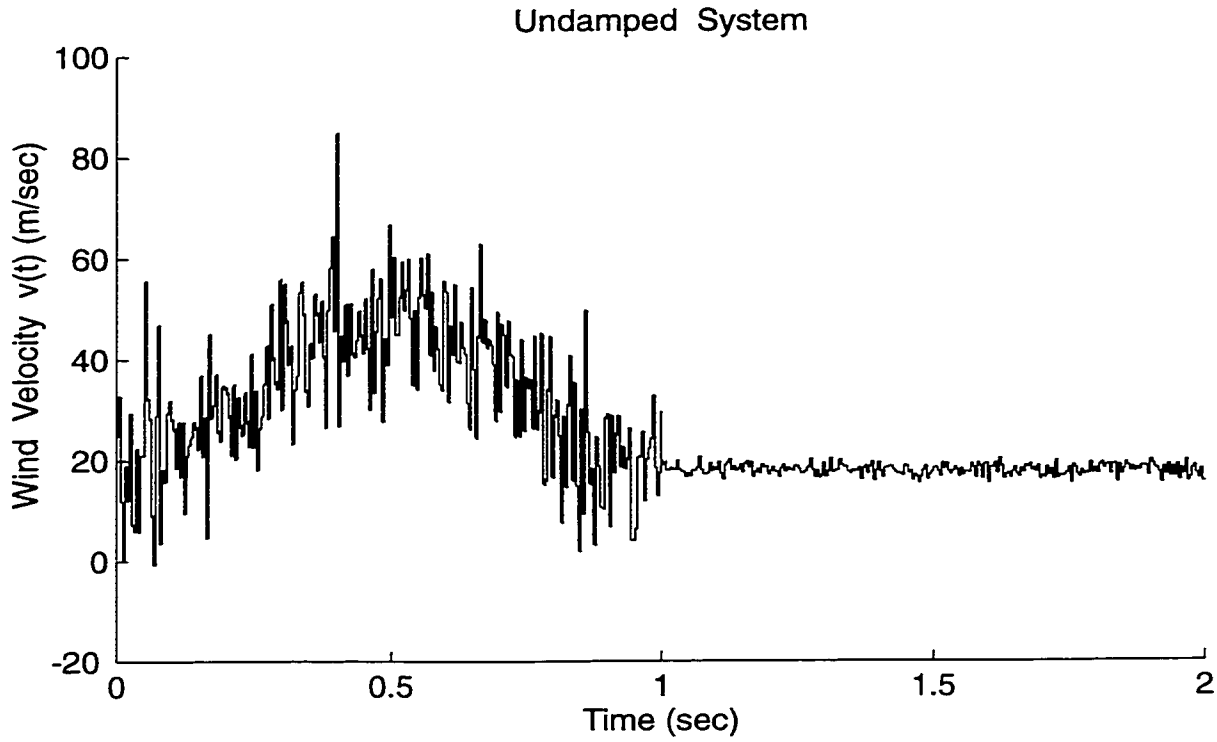
Undamped System
Wind Velocity v(t) (m/sec)
100
80
60
40
20
0
-20
0
0.5
1
1.5
2
Time (sec)

(a)

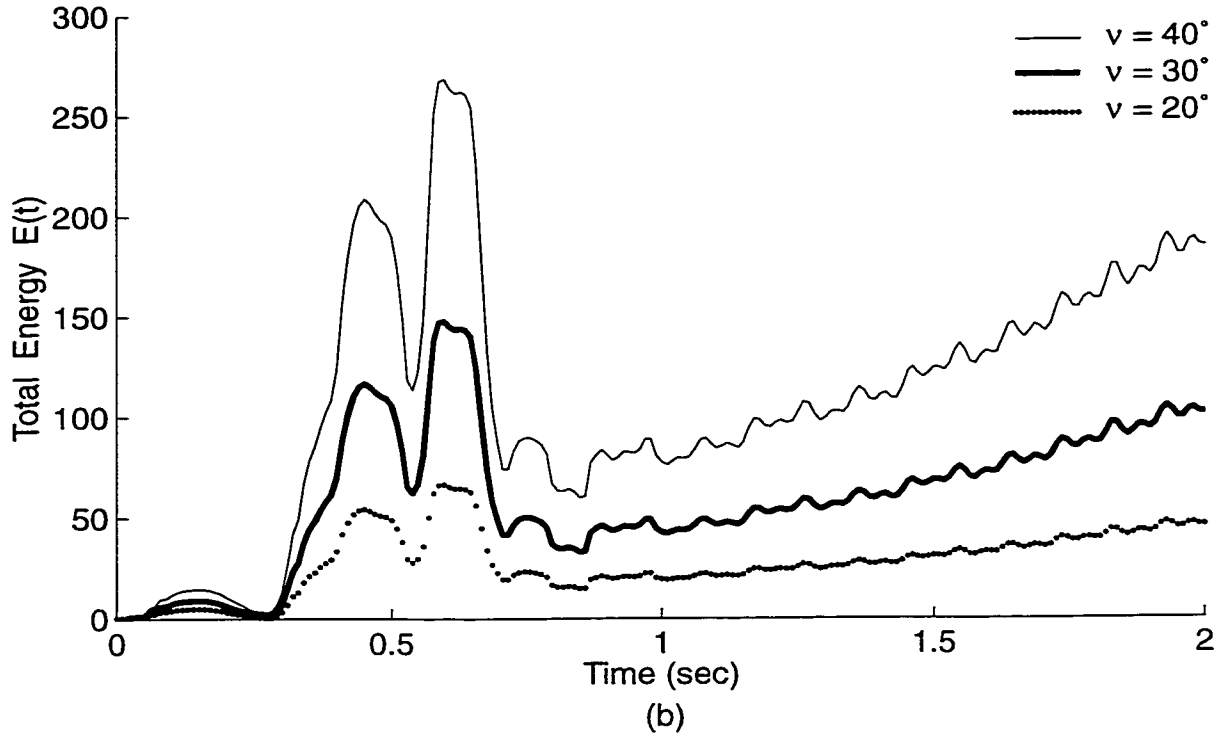
Total Energy E(t)
300
250
200
150
100
50
0
0
0.5
1
1.5
2
Time (sec)
ν = 40°
ν = 30°
ν = 20°

(b)

Figure 4.1

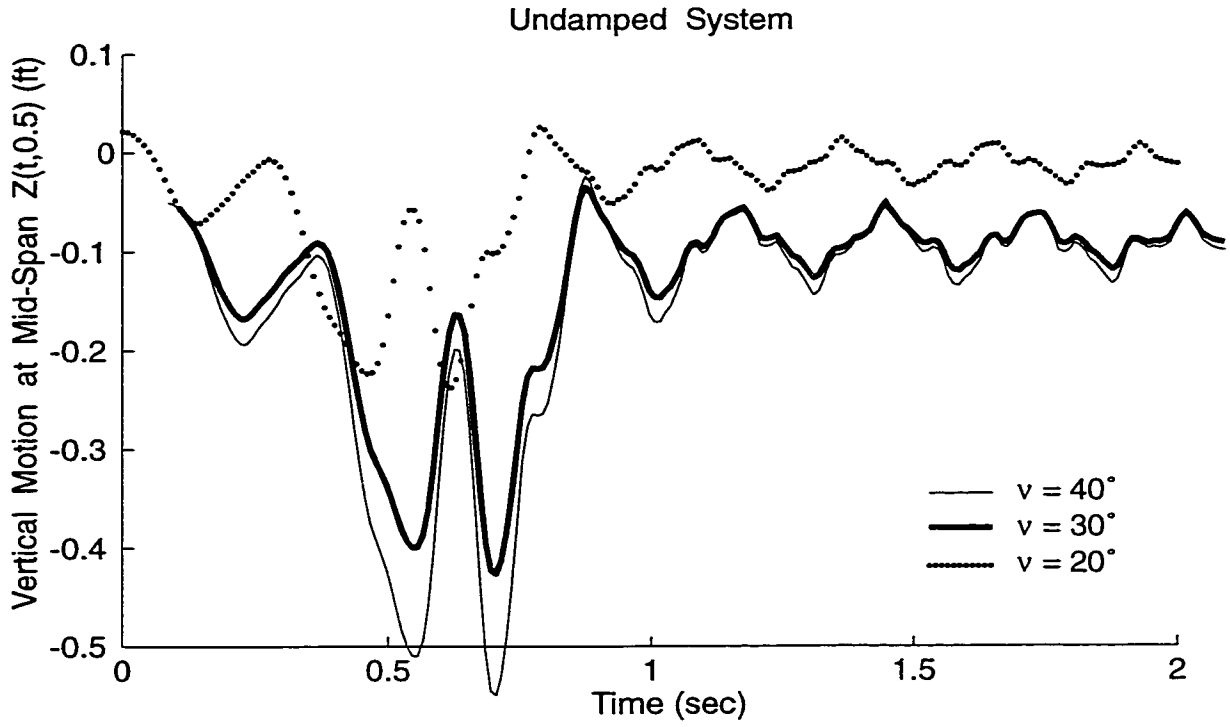
Undamped System
Vertical Motion at Mid-Span Z(t,0.5) (ft)
0.1
0
-0.1
-0.2
-0.3
-0.4
-0.5
0
0.5
1
1.5
2
Time (sec)
ν = 40°
ν = 30°
ν = 20°

(a)

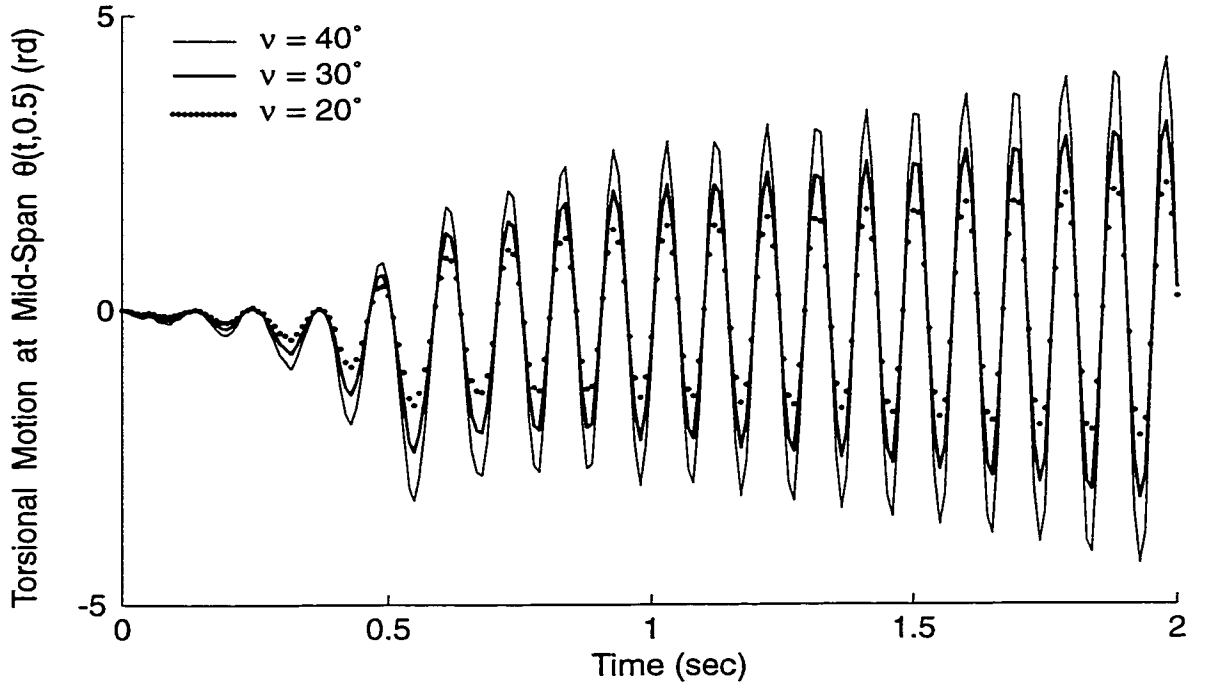
Torsional Motion at Mid-Span θ(t,0.5) (rd)
5
0
-5
0
0.5
1
1.5
2
Time (sec)
ν = 40°
ν = 30°
ν = 20°

(b)

Figure 4.2

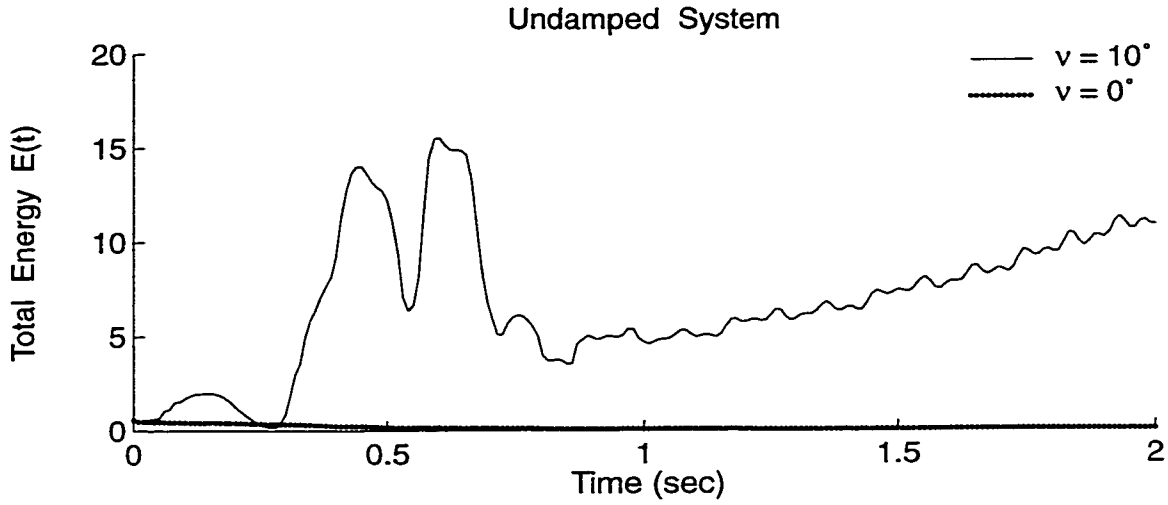

(a)

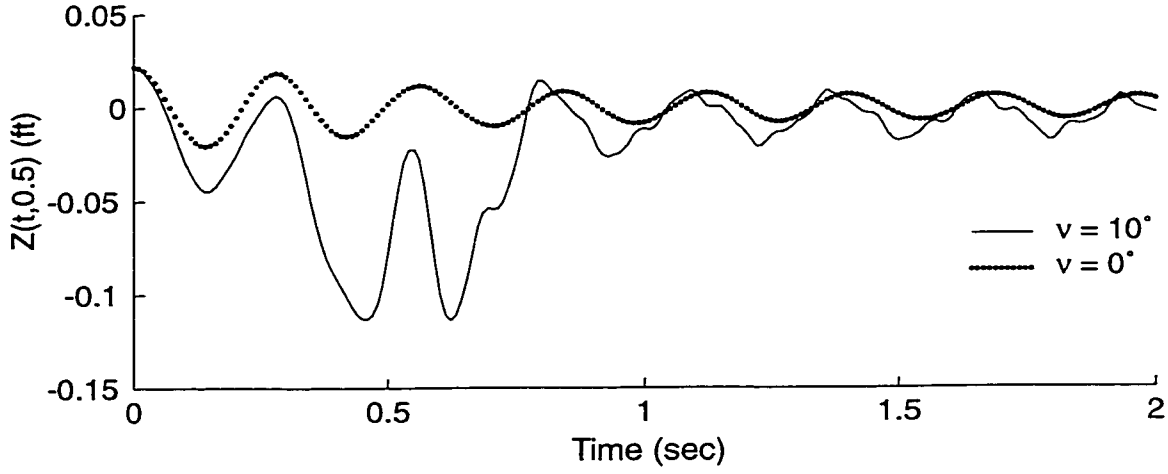

(b)

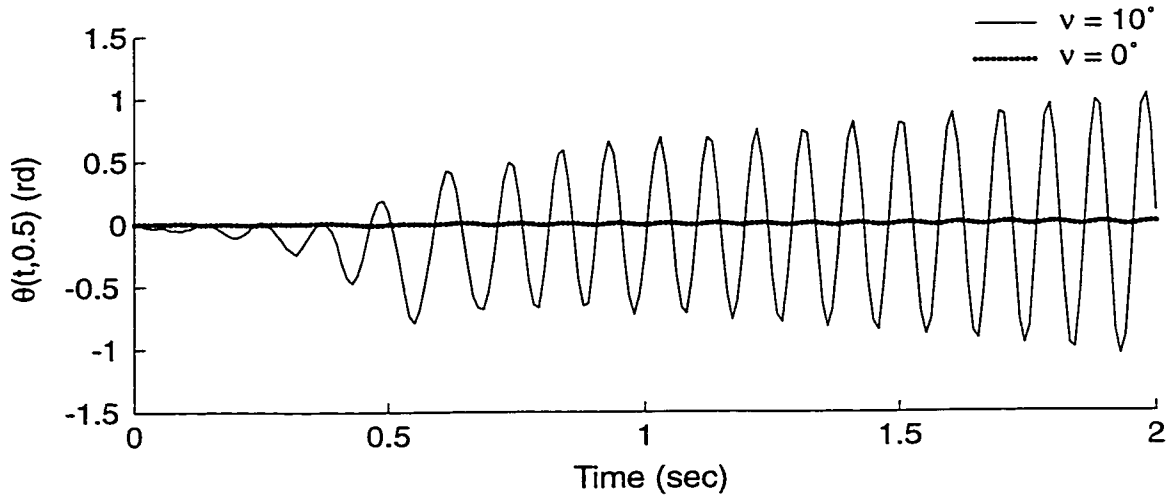

(c)

Figure 4.3

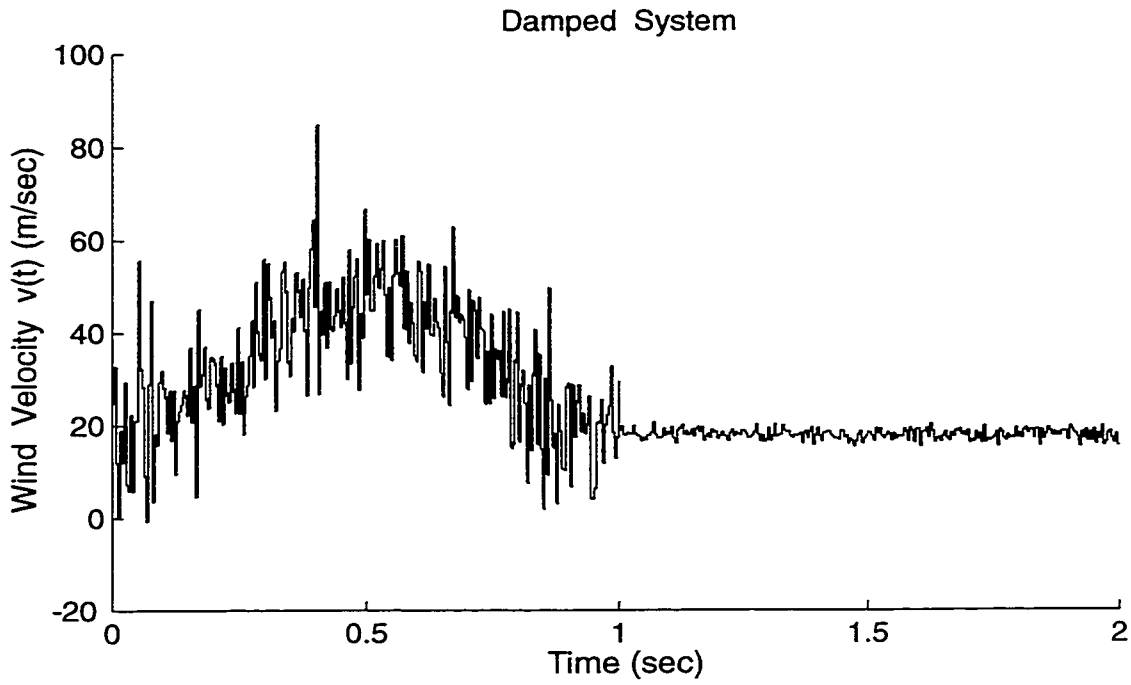
Damped System
Wind Velocity v(t) (m/sec)
100
80
60
40
20
0
-20
0
0.5
1
1.5
2
Time (sec)

(a)

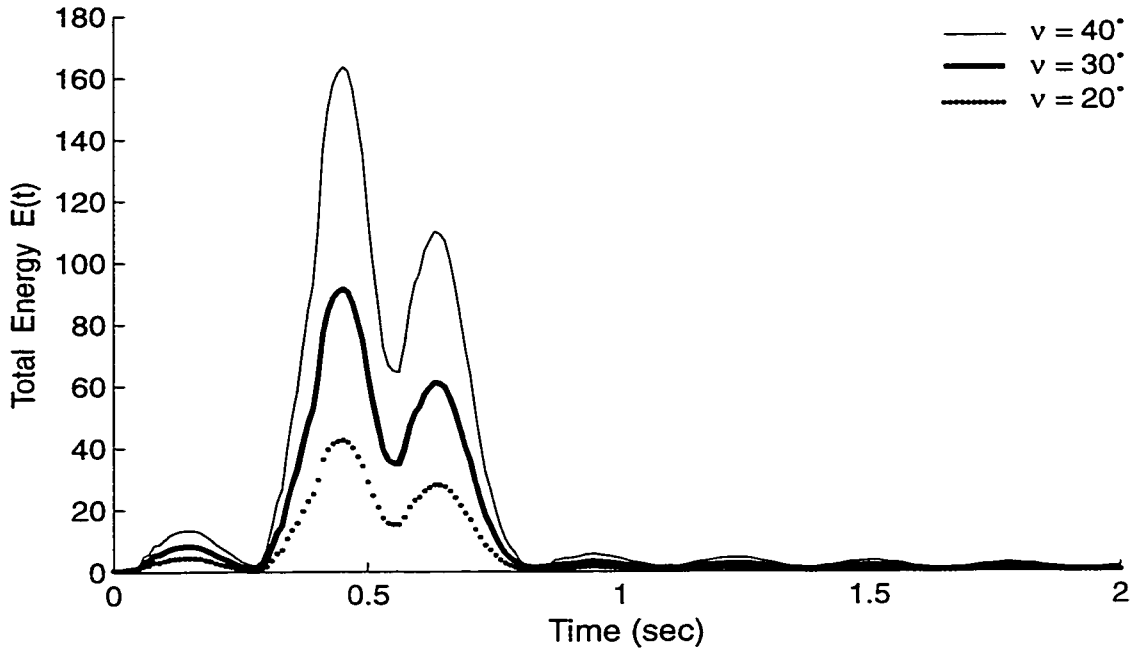
Total Energy E(t)
180
160
140
120
100
80
60
40
20
0
0
0.5
1
1.5
2
Time (sec)
ν = 40°
ν = 30°
ν = 20°

(b)

Figure 4.4

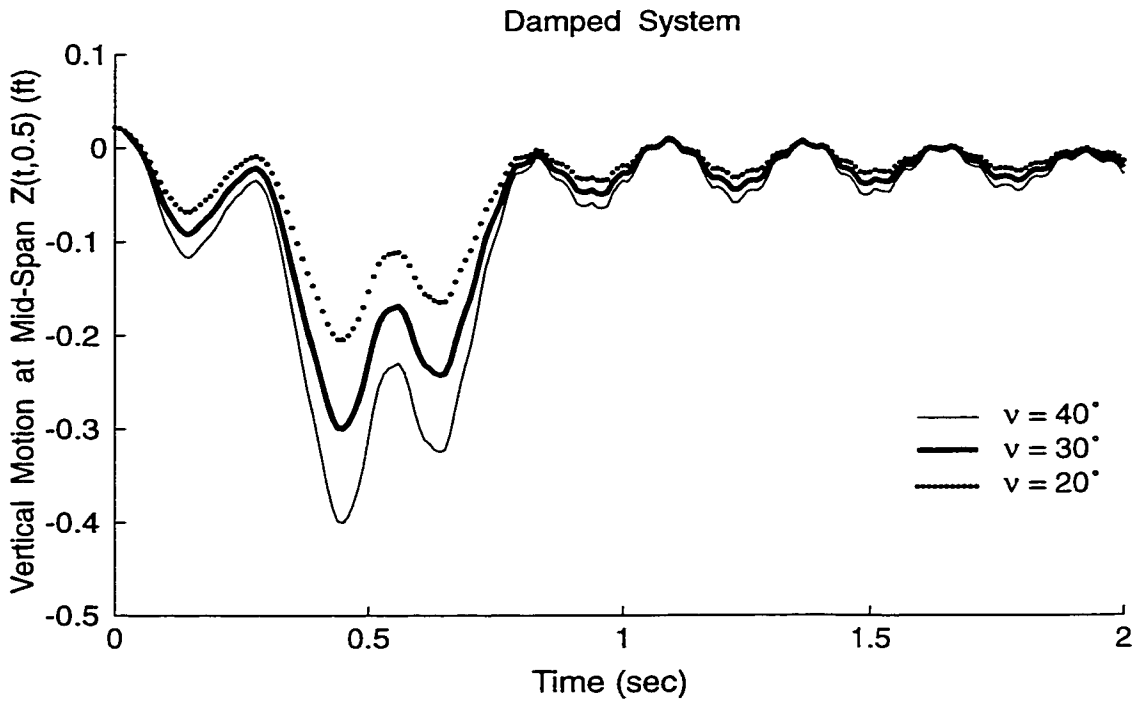
Damped System
Vertical Motion at Mid-Span Z(t,0.5) (ft)
0.1
0
-0.1
-0.2
-0.3
-0.4
-0.5
0
0.5
1
1.5
2
Time (sec)
ν = 40°
ν = 30°
ν = 20°

(a)

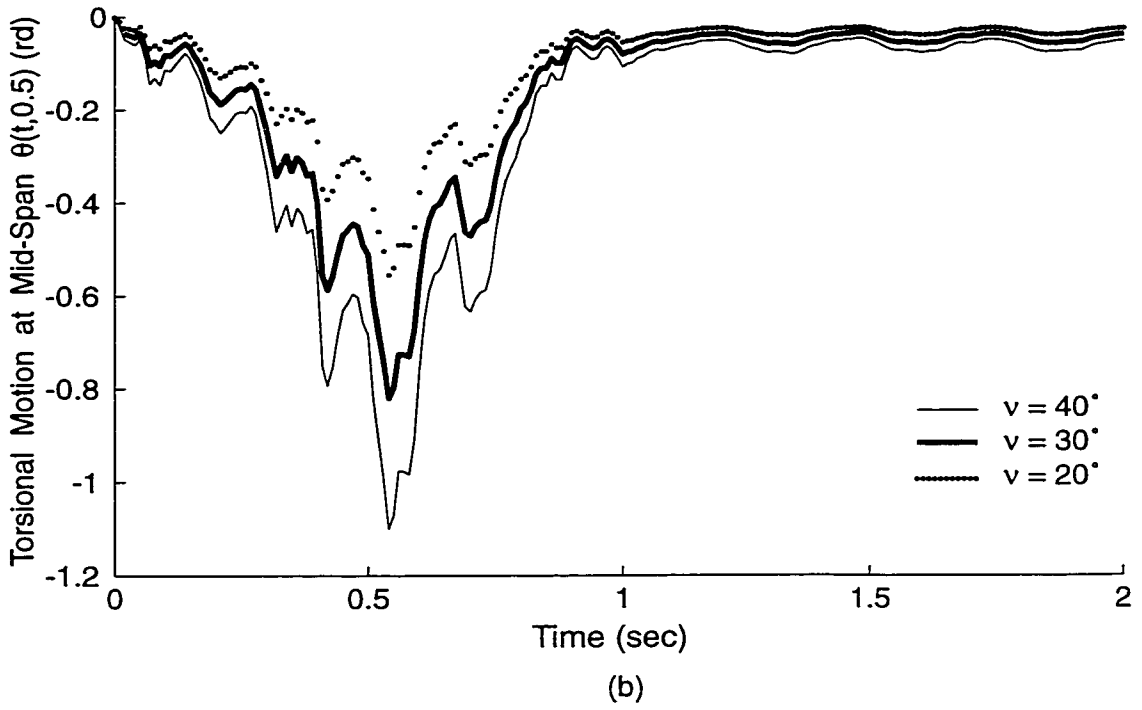
Torsional Motion at Mid-Span θ(t,0.5) (rd)
0
-0.2
-0.4
-0.6
-0.8
-1
-1.2
0
0.5
1
1.5
2
Time (sec)
ν = 40°
ν = 30°
ν = 20°

(b)

Figure 4.5

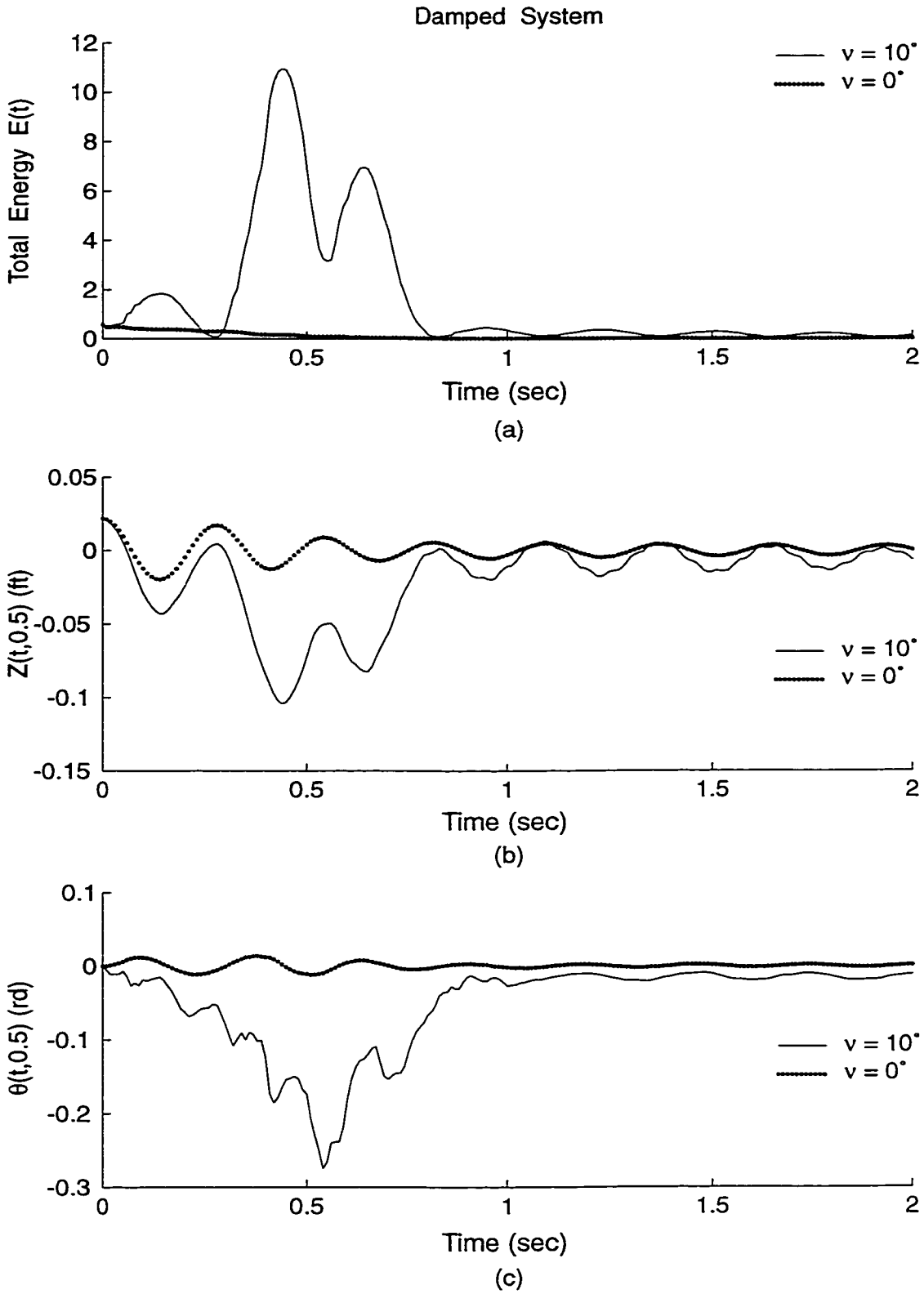
Damped System
Total Energy E(t)
Time (sec)
ν = 10°
ν = 0°
(a)
Z(t,0.5) (ft)
Time (sec)
ν = 10°
ν = 0°
(b)
θ(t,0.5) (rd)
Time (sec)
ν = 10°
ν = 0°
(c)

Figure 4.6

Chapter 5

Plate Model For Suspension Bridge

5.1 General

The exact theory of vibration in suspension bridge involves difficulties similar to. those of the deflection theory for static loads. They arise from the fact that deflections of the cable are not exactly proportional to the loads. leading to non-linear equations for additional deflections from additional forces. In order to make the problem tractable. the equations may be linearized by assuming small deflections from the initial position and neglecting second and higher order terms. Certain additional simplifying assumptions are made to facilite the solution.

5.2 System Model

For modelling the system we use the ideas of Meirovitch [34], Ahmed and Harbi [16], Lazer and McKenna [10], Timoshenko with Young and Weaver [40], Avalos and Lasiecka [39]. Combining their ideas, an approximate model is given by the following system of partial differential equations:

$$\begin{cases} m_c\dfrac{\partial^2 z_1}{\partial t^2} - \alpha\dfrac{\partial^2 z_1}{\partial x^2} + F_0(z_1 - w_{(+b/2)}) = f_1,\ x \in (0,\ell),\ t \geq 0,\ w_{(+b/2)} = w(t,x,+b/2) \\ \rho h\dfrac{\partial^2 w}{\partial t^2} + \beta\left(\dfrac{\partial^4 w}{\partial x^4} + 2\dfrac{\partial^4 w}{\partial x^2 \partial y^2} + \dfrac{\partial^4 w}{\partial y^4}\right) - H(t,x,y,z_1,z_2,w,) = f,\ \ (x,y) \in \Omega, \\ m_c\dfrac{\partial^2 z_2}{\partial t^2} - \alpha\dfrac{\partial^2 z_2}{\partial x^2} + F_0(z_2 - w_{(-b/2)}) = f_2,\ x \in (0,\ell),\ t \geq 0,\ w_{(-b/2)} = w(t,x,-b/2) \end{cases} \tag{5.1}$$

Where Ω is a closed convex domain in two dimensions and $\partial\Omega$ is its boundary. The first and the third equations describe the vibration of the main cables in vertical plain from which the road bed is suspended by stay cables (hungger cables) and the second equation describes the vertical deflection of the "middle surface" of the plate (deck) from the rest position. Here m_c is the masse per unit length of the cables, ℓ its length, α its coefficient of tensile strength, h is the uniform plate (deck) thickness, ρ its constant mass density per unit of surface area, and $\beta = \dfrac{Eh^3}{12(1-\nu^2)}$ its constant flexural rigidity, where E is Young's modulus and ν is Poisson's ratio $(0 < \nu < \dfrac{1}{2})$. The functions F_0 and H represent the restraining forces experienced by the road bed and the suspension cables as transmited through the stay lines. Thus functions produce the coupling. The functions f_1 , f_2 and f represent external as well as non-conservative forces, which are generally time-dependent acting on the system.

In order to solve the system of equations (5.1), one must provide the boundary and initial conditions for z_1 , z_2 and w .

5.2.1 Boundary Conditions

For all $t \geq 0$, we assume that the middle section is clamped to the bays at both ends. The boundary conditions are given by:

$$\begin{cases} z_1(x,t) = 0, & \text{at } x = 0,\ x = \ell, \\ z_2(x,t) = 0, & \text{at } x = 0,\ x = \ell, \end{cases} \tag{5.2}$$

$$\begin{cases} w(x,y,t) = 0, & \text{at } x = 0,\ x = \ell, \\ \dfrac{\partial w}{\partial x}(x,y,t) = 0, & \text{at } x = 0,\ x = \ell, \end{cases} \tag{5.3}$$

and

$$\begin{cases} \left(\nu\dfrac{\partial^2 w}{\partial x^2} + \dfrac{\partial^2 w}{\partial y^2}\right) = 0. & \text{at } y = \pm b/2 \\ \left(\dfrac{\partial^3 w}{\partial y^3} + (2-\nu)\dfrac{\partial^3 w}{\partial x^2 \partial y}\right) = 0, & \text{at } y = \pm b/2. \end{cases} \tag{5.4}$$

5.2.2 Initial Conditions

The initial conditions are given by

$$\begin{cases} z_1(x,t) = h_1(x), \quad \dfrac{\partial z_1}{\partial t}(x,t) = 0, & \text{at } t = 0, \ \forall x \in \Sigma = (0,\ell) \\ z_2(x,t) = h_2(x), \quad \dfrac{\partial z_2}{\partial t}(x,t) = 0, & \text{at } t = 0, \ \forall x \in \Sigma = (0,\ell) \end{cases} \tag{5.5}$$

for the suspension cables and by:

$$\begin{cases} w(x,y,t) = h(x,y), & \text{at } t = 0, \ \forall (x,y) \in \Omega, \\ \dfrac{\partial w}{\partial t}(x,y,t) = 0, & \text{at } t = 0, \ \forall (x,y) \in \Omega \end{cases} \tag{5.6}$$

for the suspended structure, where $\{h_1, h_2\}$ and h are suitable real valued functions defined respectively in the domains $\Sigma = (0,\ell)$ and Ω, respectively.

5.3 An Explicit Method for the Plate Equation

Almost everything said in the previous chapters about finite difference solution of one-dimensional suspension bridge problems is generalized in to more than one space dimension. Since it was seen that the lower-order terms in the partial differential equations do not affect the stability, and since it will be clear how to treat more general problems, including three-dimensional problems, we will limit our study to the simple dynamical Kirchhoff plate equation.

5.4 Governing Equation

Here we consider a clamped - free square plate of side ℓ that is subjected to a load $g(x, y, t)$ per unit area, as shown in Figure 5.1. The deflection w in the z-direction is the solution of the two-dimensional clamped-free vibratrion plate problem, normalezed in the form

$$\frac{\partial^2 w}{\partial t^2} + \frac{\partial^4 w}{\partial x^4} + 2\frac{\partial^4 w}{\partial x^2 \partial y^2} + \frac{\partial^4 w}{\partial y^4} = g(x, y, t), \quad (x, y) \in \Omega, \quad t \geq 0 \tag{5.7}$$

subject to the boundary conditions explained in the subsection below.

5.4.1 Boundary Contions

A complete solution of the governing equation (5.7) depends upon the knowledge of the conditions of the plate at the boundaries in terms of the lateral deflection of the middle $w(x, y)$ at a given time t. Thus, expressions for these conditions must be developped. Two types of boundaries are considered: clamped and free.

- **Clamped Edge Conditions.**

For the clamped boundary of the plate, the deflection w and the slope $\dfrac{\partial w}{\partial x}$ of the middle surface must vanish at the boundary. On the clamped edges parallel to the y axis at $x = 0$

and $x = \ell$, Figure 5.1, the boundary conditions are

$$\begin{cases} w|_{x=0} = w|_{x=\ell} = 0, \\ \dfrac{\partial w}{\partial x}\Big|_{x=0} = \dfrac{\partial w}{\partial x}\Big|_{x=\ell} = 0. \end{cases} \tag{5.8}$$

- **Free Edge Conditions.**

In the most general case, the bending moment M_y and the tranverse shear force V_{yz} acting on the free edge of the plate must vanish. The boundary conditions on the free edges parallel to the x axis at $y = 0$ and $y = \ell$, Figure 5.1, are

$$\begin{cases} \left(\nu\dfrac{\partial^2 w}{\partial x^2} + \dfrac{\partial^2 w}{\partial y^2}\right)\Big|_{y=0} = \left(\nu\dfrac{\partial^2 w}{\partial x^2} + \dfrac{\partial^2 w}{\partial y^2}\right)\Big|_{y=\ell} = 0, \\ \left(\dfrac{\partial^3 w}{\partial y^3} + (2-\nu)\dfrac{\partial^3 w}{\partial x^2 \partial y}\right)\Big|_{y=0} = \left(\dfrac{\partial^3 w}{\partial y^3} + (2-\nu)\dfrac{\partial^3 w}{\partial x^2 \partial y}\right)\Big|_{y=\ell} = 0. \end{cases} \tag{5.9}$$

5.4.2 Initial Conditions

$$\begin{cases} w(x, y, t) = h(x, y), \quad \text{at} \quad t = 0, \quad \forall (x, y) \in \Omega, \\ \dfrac{\partial w}{\partial t}(x, y, t) = 0, \quad \text{at} \quad t = 0, \quad \forall (x, y) \in \Omega \end{cases} \tag{5.10}$$

5.4.3 Method of Solution

A natural way to discretize (5.7) is to use the centered difference formula, for which a rectangular grid is marked off in the unit square by using the grid lines

$$x_i = i\Delta x \qquad \left(\Delta x = \frac{1}{N}\right)$$

$$y_j = j\Delta x \qquad \left(\Delta y = \frac{1}{M}\right)$$

and we likewise define

$$t_k = k\Delta t.$$

To approximate the partial differential equation (5.7), we have to discretize the biharmonic equation (the first member of (5.7)) on a uniform grid using a 13-point approximation with truncation error of order h^2, an explicit finite difference discretization at a grid point (x_i, y_j) may be written as; for $i = 2, ..., N, J = 1, ..., N+1$:

$$\frac{1}{\Delta t^2}\Big[w(x_i, y_j, t_{k+1}) - 2w(x_i, y_j, t_k) + w(x_i, y_j, t_{k-1})\Big] = g(x_i, y_j, t_k)$$

$$-\frac{1}{\Delta x^4}\Big[(x_{i+2}, y_j, t_k) - 4w(x_{i+1}, y_j, t_k) + 6w(x_i, y_j, t_k) - 4w(x_{i-1}, y_j, t_k) + w(x_{i-2}, y_j, t_k)\Big]$$

$$-\frac{1}{\Delta y^4}\Big[w(x_i, y_{j+2}, t_k) - 4w(x_i, y_{j+1}, t_k) + 6w(x_i, y_j, t_k) - 4w(x_i, y_{j-1}, t_k) + w(x_i, y_{j-2}, t_k)\Big]$$

$$-\frac{1}{\Delta x^2 \Delta y^2}\Big[w(x_{i+1}, y_{j+1}, t_k) - 2w(x_i, y_{j+1}, t_k) + w(x_{i-1}, y_{j+1}, t_k) - 2w(x_{i+1}, y_j, t_k) \qquad (5.11)$$

$$+ 4w(x_i, y_j, t_k) - 2w(x_{i-1}, y_j, t_k) + w(x_{i+1}, y_{j-1}, t_k) - 2w(x_i, y_{j-1}, t_k) + w(x_{i-1}, y_{j-1}, t_k)\Big]$$

with

$$\begin{cases} w(x_i, y_j, t_0) = h(x_i, y_j), \\ \\ w(x_i, y_j, t_1) = h(x_i, y_j) + \frac{1}{2}\Delta t^2\Big[g(x, y, t_0) - \Delta^2 w(x, y, t_0)\Big], \end{cases} \qquad (5.12)$$

and $w(x_i, y_j, t_k)$ must satisfy the boundary conditions when (x_i, y_j) on the boundary.

For the clamped edges parallel to the y axis, the finite difference approximations of the boundary conditions $w = 0$ and $\dfrac{\partial w}{\partial x} = 0$ are:

$$\begin{cases} w(x_1, y_j, t_k) = w(x_{N+1}, y_j, t_k) = 0, & \text{for } j = 1, ..., N+1 \\ w(x_0, y_j, t_k) = w(x_2, y_j, t_k), \quad w(x_{N+2}, y_j, t_k) = w(x_N, y_j, t_k) & \text{for } j = 1, ..., N+1 \end{cases} \tag{5.13}$$

For the free edges parallel to the x axis, the boundary conditions are $M_y = V_{yz} = 0$. The finite difference approximations of $M_y = 0$, obtained from the first equation in the system (5.9), are, for $i = 2, ..., N$:

$$\begin{cases} w(x_i, y_2, t_k) + w(x_i, y_0, t_k) + \nu w(x_{i+1}, y_1, t_k) \\ \qquad +\nu w(x_{i-1}, y_1, t_k) - (2 + 2\nu) w(x_i, y_1, t_k) = 0, \\ \\ w(x_i, y_{N+2}, t_k) + w(x_i, y_N, t_k) + \nu w(x_{i+1}, y_{N+1}, t_k) \\ \qquad +\nu w(x_{i-1}, y_{N+1}, t_k) - (2 + 2\nu) w(x_i, y_{N+1}, t_k) = 0. \end{cases} \tag{5.14}$$

The finite difference approximations of $V_{yz} = 0$, obtained from the second equation in the system (5.9), are, for $i = 2, ..., N$:

$$\begin{cases} w(x_i, y_3, t_k) - 2(3 - \nu) w(x_i, y_2, t_k) + 2(3 - \nu) w(x_i, y_0, t_k) - w(x_i, y_{-1}, t_k) \\ \qquad +(2 - \nu) w(x_{i+1}, y_2, t_k) + (2 - \nu) w(x_{i-1}, y_2, t_k) \\ \qquad -(2 - \nu) w(x_{i+1}, y_0, t_k) - (2 - \nu) w(x_{i-1}, y_0, t_k) = 0, \end{cases} \tag{5.15}$$

and

$$\begin{cases} w(x_i, y_{N+3}, t_k) - 2(3 - \nu) w(x_i, y_{N+2}, t_k) + 2(3 - \nu) w(x_i, y_N, t_k) - w(x_i, y_{N-1}, t_k) \\ \qquad +(2 - \nu) w(x_{i+1}, y_{N+2}, t_k) + (2 - \nu) w(x_{i-1}, y_{N+2}, t_k) \\ \qquad -(2 - \nu) w(x_{i+1}, y_N, t_k) - (2 - \nu) w(x_{i-1}, y_N, t_k) = 0. \end{cases} \tag{5.16}$$

The continuity of zero curvature, gives us four equations. We know that the plate is flat along the clamped edges at $x = 0$ and $x = \ell$. Thus, we have the following four expressions

$$\begin{cases} w(x_1, y_{-1}, t_k) = -w(x_1, y_2, t_k), & w(x_{N+1}, y_{-1}, t_k) = -w(x_{N+1}, y_2, t_k), \quad \forall t > 0 \\ w(x_1, y_{N+2}, t_k) = -w(x_1, y_N, t_k), & w(x_{N+1}, y_{N+2}, t_k) = -w(x_{N+1}, y_N, t_k), \quad \forall t > 0 \end{cases} \tag{5.17}$$

Since $w(x_1, y_2, t_k) = w(x_{N+1}, y_2, t_k) = w(x_1, y_N, t_k) = w(x_{N+1}, y_N, t_k) = 0$, these four expressions reduce to

$$\begin{cases} w(x_1, y_{-1}, t_k) = 0, \\ w(x_{N+1}, y_{-1}, t_k) = 0, \\ w(x_1, y_{N+2}, t_k) = 0, \\ w(x_{N+1}, y_{N+2}, t_k) = 0. \end{cases} \tag{5.18}$$

The values of w at $t = t_1$ were estimated using Taylor series as follows:

$$\begin{cases} w(x, y, \Delta t) \approx w(x, y, 0) + \Delta t w_t(x, y, 0) + \frac{1}{2}\Delta t^2 w_{tt}(x, y, 0) \\ \quad = w(x, y, 0) + 0 + \frac{1}{2}\Delta t^2 \Big[g(x, y, 0) - \Delta^2 w(x, y, 0) \Big] \\ \quad = h(x, y) + \frac{1}{2}\Delta t^2 \Big[g(x, y, 0) - h_{xxxx}(x, y) - 2h_{xxyy}(x, y) - h_{yyyy}(x, y) \Big] \end{cases} \tag{5.19}$$

5.4.4 Example

In this subsection, we present some simulation results given by Figure 5.2. We shall direct ourselves to the problem of determining the lateral deflections of the rectangular plate. Figure 5.1 shows the typical geometry of clamped-free plate which is self explanatory. To

apply the equations shown previously, we solve a problem by the centred difference method using a explicit scheme,(see [35, 36, 37, 38]). The size of time steps and space steps that were used have been found to be sufficiently small to give highly accurate results. For the purpose of the simulation, we assume that the plate is uniform. We used the following parameters: (as suggesting in reference [41]):

$$\ell = 1.0, \quad \nu = 0.3$$

$$\frac{\partial^2 w}{\partial t^2} + \frac{\partial^4 w}{\partial x^4} + 2\frac{\partial^4 w}{\partial x^2 \partial y^2} + \frac{\partial^4 w}{\partial y^4} = 0, \quad (x, y) \in \Omega, \quad t \geq 0 \tag{5.20}$$

with the boundary conditions:

$$\begin{cases} w|_{x=0} = w|_{x=\ell} = 0, \\ \dfrac{\partial w}{\partial x}\Big|_{x=0} = \dfrac{\partial w}{\partial x}\Big|_{x=\ell} = 0. \end{cases} \tag{5.21}$$

for the clamped edges and

$$\begin{cases} \left(\nu\dfrac{\partial^2 w}{\partial x^2} + \dfrac{\partial^2 w}{\partial y^2}\right)\Big|_{y=0} = \left(\nu\dfrac{\partial^2 w}{\partial x^2} + \dfrac{\partial^2 w}{\partial y^2}\right)\Big|_{y=\ell} = 0, \\ \left(\dfrac{\partial^3 w}{\partial y^3} + (2-\nu)\dfrac{\partial^3 w}{\partial x^2 \partial y}\right)\Big|_{y=0} = \left(\dfrac{\partial^3 w}{\partial y^3} + (2-\nu)\dfrac{\partial^3 w}{\partial x^2 \partial y}\right)\Big|_{y=\ell} = 0. \end{cases} \tag{5.22}$$

for the free edges, and with the following initial conditions:

$$\begin{cases} w(x, y, t) = h(x, y), \quad \text{at} \quad t = 0, \quad \forall (x, y) \in \Omega, \\ \dfrac{\partial w}{\partial t}(x, y, t) = 0, \quad \text{at} \quad t = 0, \quad \forall (x, y) \in \Omega \end{cases} \tag{5.23}$$

where

$$\begin{cases} h(x,y) = X(x)Y(y) \\ X(x) = cosh(\lambda x) - cos(\lambda x) - \dfrac{cosh(\lambda) - cos(\lambda)}{sinh(\lambda) - sin(\lambda)}\Big[sinh(\lambda x) - sin(\lambda x)\Big], \\ Y(y) = cosh(\lambda y) + cos(\lambda y) - \dfrac{cosh\lambda) - cos(\lambda)}{sinh(\lambda) - sin(\lambda)}\Big[sinh(\lambda y) + sin(\lambda y))\Big], \end{cases} \tag{5.24}$$

Where $X(x)$ and $Y(y)$ represent the first mode of vibration for a clamped-clamped and free-free beams respectively, with λ satisfying $coh(\lambda)cos(\lambda) = 1$.

The finite difference approximation of the governing differential equation, given by equation (5.11), must be applied to all points on the plate except for those on the clamped boundaries. At those points on the clamped boundaries, equilibrium is satisfied by the condition that $w = 0$. Thus, equation (5.11) must be applied to all interior points and also to the points on the free edges.

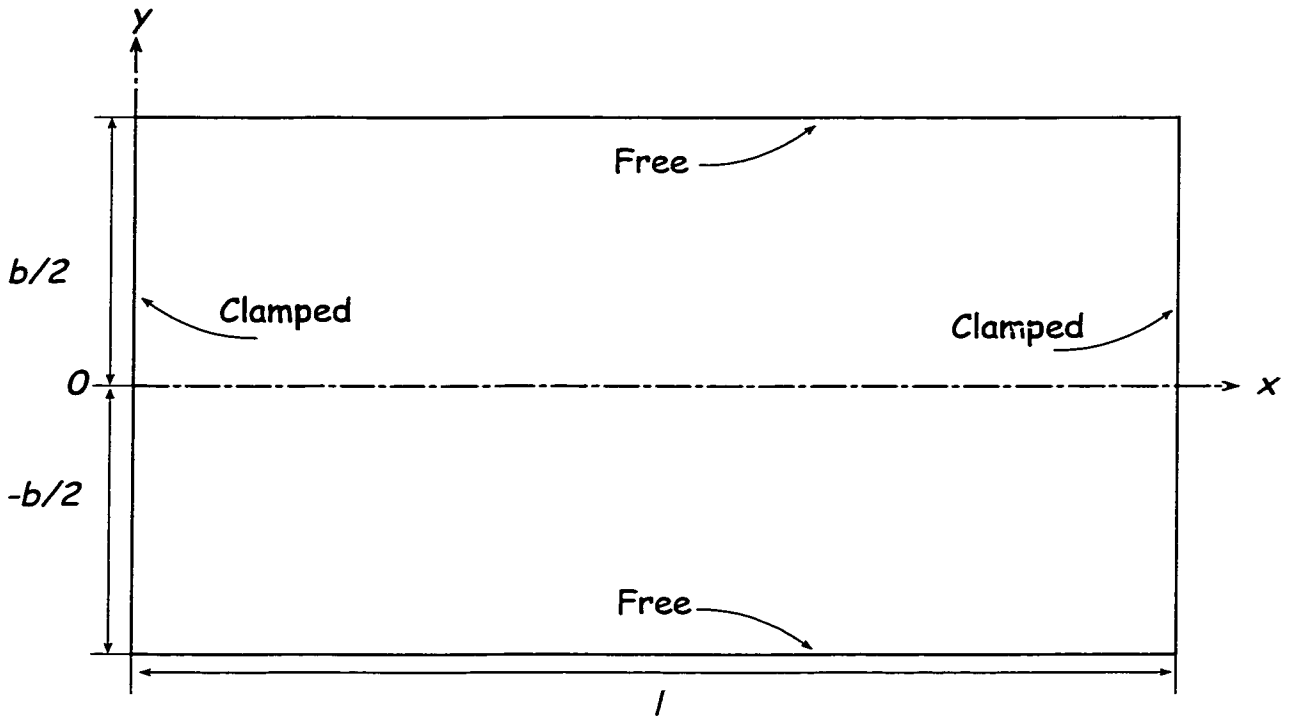

FIGURE 5.1 Kirchhoff plate representation of beam-slab type highway bridge.

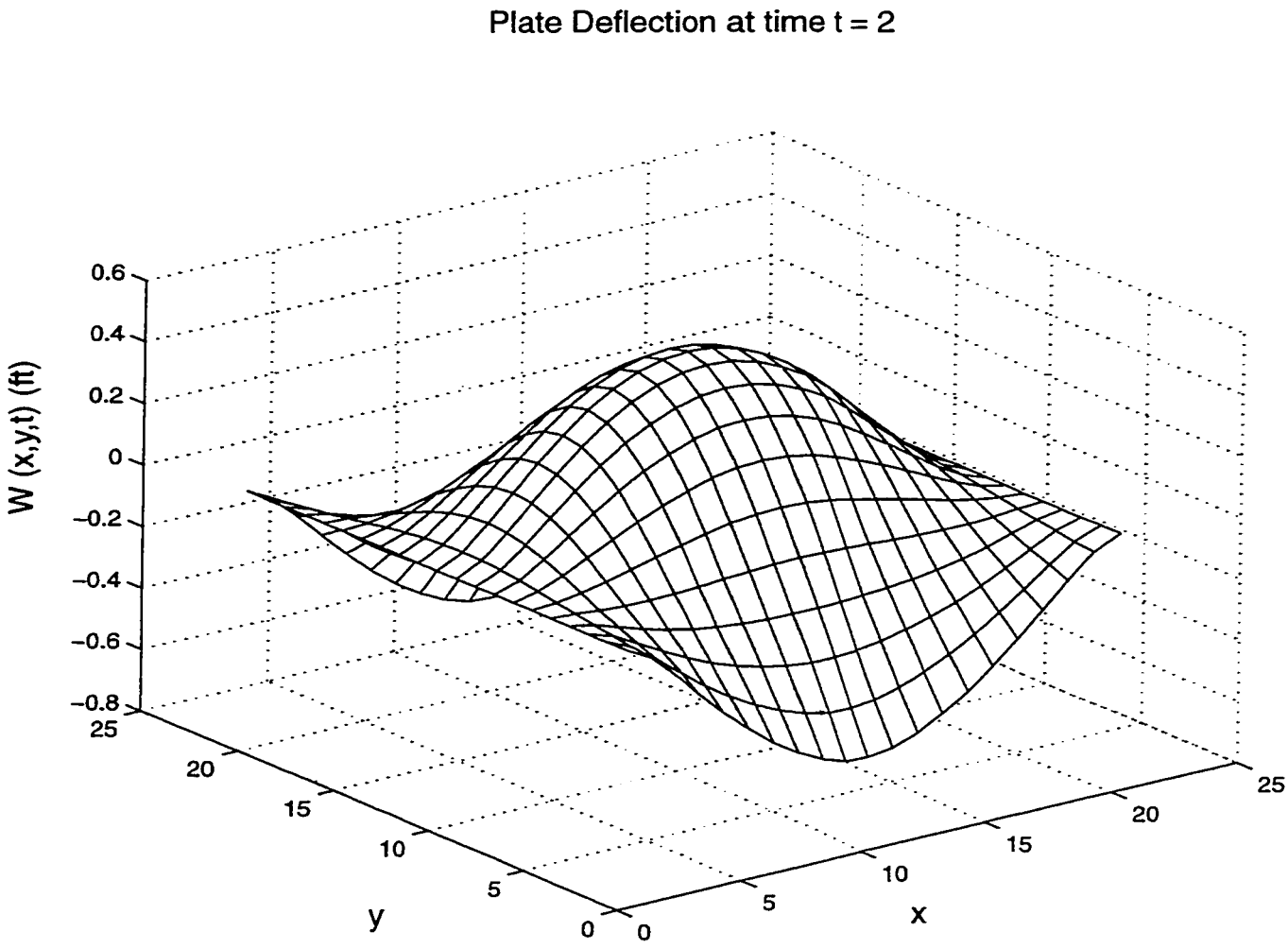

FIGURE 5.2 Finite Difference Solutions fora the Lateral Deflections of Plate

Chapter 6

Conclusions and Suggestions for Further Research

6.1 Conclusions

The objective of this thesis is to study the dynamic & stability of suspension bridges. The following are the main conclusions drawn from this study. In chapter 2 and 3, we have presented a few dynamic models of suspension bridges described by a system of hyperbolic parial differential equations with linear and nonliear couplings. In chapter 2, we study analytically the stability properties of the system. We have provided numerical results illustrating the comparative effectiveneess of aerodynamic and structural damping. Increasing either of these damping coefficients indefinitely does not necessarily increase the decay rate indefinitely. There is an optimum value for these parameters.

In chapter 3 we develop a dynamic model of suspension bridge governed by a system of coupled hyperbolic partial differential equations which provide both torsional and vertical motion of the roadway. The coupling between the two motions is a nonlinear operation arising from the loss of tension in the stays cables supporting the deck. We study the impact of the wind forces in presence and absence of aerodynamic and strutural damping on the stability of this system. The results are illustrated by numerical simulation.

In chapter 4 we introduce and study the stochastic versions of the model (B) as developed in chapter 3. The results are illustrated by numerical simulation for the model of suspension bridges subject to stochastic wind load.

In this chapter we consider the problem of stability of suspension bridges in the presence of random wind forces acting on the deck and the suspension cables. Total mechanical energy given by the sum of all kinetic and elastic potential energies of the structure, is used as a Lyapunov functional. Assuming negligible mechanical friction and viscous damping, it is seen that the system is conservative and that random wind forces can destabilize the system. In the presence of structural damping, provided by piezo ceramic layers or other smart materials, it is seen that the system is asymptotically stable. This is clearly illustrated by numerical results presented in the final section of the chapter.

In chapter 5 we have presented a dynamic model of suspension bridge based on plate model as road way. The predictions from this model are more realistic since the behaviour of the road bed is simulated in the two directions.

6.2 Suggestion for Further Work

As a continuation to this study, further research could be carried out along the following directions:

- A more elaborate model such as the one given by (5.1) and its stochastic version including simulation is still needed.
- A study of the nonlinear torsional vibration of two-dimensional suspension bridge is essential.
- Better ways to find large amplitude solutions including continuation and variational methods. None of these methods have been applied to the coupled cables-plate equations. A really interesting problem will be to see the solution to the full system of partial differential

equations as given in chapter 5 $\{(5.1), ..., (5.6)\}$ with the appropriate couplings.

- Future work should also focus on developing guidelines to control stability of suspension bridges.

Bibliography

[1] O.H.Amann, T.Von Karman, and G.B. Woodruff; The Failure of the Tacoma Narrows Bridge, Federal Works Agency, 1941.

[2] F.Bleich, C.B.McCullough, R.Rosecrans, and G.S.Vincent; The Mathematical Theory of Suspension Bridges. U.S. Dept. of Commerce, Bureau of Public Roads, 1950.

[3] E.G.Wiles, "Report of Aerodynamic Studies on Proposed San Pedro-Terminal Island Suspension Bridge, California," Bridge Research Branch, Division of Physical Research, Bureau of Public Roads, U.S. Dept.of Commerce, Washington, D.C., 1960.

[4] A.Selberg, Oscillation and Aerodynamic Stability of Suspension Bridges, Acta Polytechnia Scandinavia, pp.308-377, 1961.

[5] A.M.Abdel-Ghaffer, Suspension Bridge Vibration: Continuum Formation, J.Engrg.Mech. 108, pp.1215-1232, 1982.

[6] T.Kawada and A.Hirai, Additional Mass Method-A New Approach to Suspension Bridge Rehabilitation, Official Proceedings, 2nd Annual International Bridge Conference. Engineers of Society of Western Pennsylvania, 1985.

[7] P.J.McKenna and W.Walter, Nonlinear Oscillation in a Suspension Bridge, Arch. Rational Mech. Anal. 98, pp.167-177, 1987.

[8] A.C.Lazer and P.J.McKenna; Large Scale Oscillation Behavior in Loaded Asymmetric Systems,Ann.Inst. H.Poincare, Analyse Nonlineaire, Vol. 4, pp.244-274, 1987.

[9] J.Glover, A.C.Lazer, and P.J.McKenna, Existence and Stability of Large Scale Nonlinear Oscillations in Suspension Bridges, Journal of Applied Mathematics and Physics (ZAMP) Vol. 40, pp.172-200, March 1989.

[10] A.C.Lazer and P.J.McKenna; Large-Amplitude Periodic Oscillations in Suspension Bridge: Some New Connections with Nonlinear Analysis, SIAM Rev. 32, pp.537-78, 1990.

[11] P.J.McKenna nd W.Walter, Traveling Waves in a Suspension Bridge, SIAM J.Appl. Math. Vol. 50, N0. 3, pp.703-715, June 1990.

[12] Y.S.Choi, K.C.Jen, and P.J.McKenna, The Structure of the Solution Set for Periodic Oscillation in a Suspension Bridge Model, IMA JournAl of Applied Mathematics Vol. 47, pp.283-306, 1991.

[13] Daniela Jacover and P.J.McKenna, Nonlinear Torsional Flexings in a Periodically Forced Suspended Beam, Journal of Computational and Applied Mathematics Vol. 52, pp.241-265, 1994.

[14] M. Roseau, Vibrations in Mechanical Systems, Springer-verlag, Berlin Heidelberg New York London Paris Tokyo, (1984).

[15] K.Y.Billah and R.H.Scanlan, Resonance, Tacoma Narrows Bridge Failure, and Undergraduate Physics Texbooks, Amer. J. Physics, Vol.**59**, No.**2**, pp.118-124 (Feb. 1991).

[16] N.U.Ahmed and H.Harbi, Mathematical Analysis of Dynamic Models of Suspension Bridge,SIAM Journal of Applied Mathematics Vol. **58 No.3**, pp.853-874, 1998.

[17] R.A. Adams, Sobolev Spaces, Academic Press, New York 1975

[18] N.U.Ahmed and H.Harbi, Dynamic Models of Suspension Bridge and their Stability, Proc. of the IASTED International Conference, Control 97, Cancun, Mexico,(May 28–31, 1997), 386-390.

[19] N.U.Ahmed and H.Harbi, Stability of Suspension Bridge I: Aerodynamic and Structural Damping, J. Mathematical Problems in Engineering, Vol. **4**, pp. 73-98, 1998.

[20] N.U.Ahmed and H.Harbi, Stability of Suspension Bridge II: Aerodynamic vs Structural Damping, Proc. of SPIE, Smart Structures and Materials 1998, Smart Systems for Bridges, Structures, and Highways, San Diego, California, pp.276-289.

[21] N.U.Ahmed and H.Harbi, Torsional and Longitudinal Vibration of Suspension Bridge Subject to Aerodynamic Forces, J. Mathematical Problems in Engineering, Vol.**3(4)**, pp.1-29, 1998.

[22] N.U.Ahmed and H.Harbi, Stochastic Modelling and Stability of Suspension Bridge Proc. of SPIE, Smart Structures and Materials 2000, Smart Systems for Bridges, Structures, and Highways, San Diego, California, pp.394-399

[23] S.K.Biswas and N.U.Ahmed, Optimal Control of Large Space Structures Governed by a Coupled System of Ordinary and Partial Differential Equations, J. Mathematics of Control, Signals, and Systems, Vol. 2, pp 1-18, 1989.

[24] N.U.Ahmed and S.S.Lim, Modeling and Control of Flexible Space Stations (Slew Maneuvers), Proceedings of the 3rd Annual Conference on Aerospace Computational Control, (Ed. D.E.Bernard and G.K.Mann),JPL, NASA Pub. 89-45, Vol. 2, pp.900-914.

[25] N.U.Ahmed and S.K.Biswas, Mathematical Modeling and Control of Large Space Structures with Multiple Appendages, J.Math Comput. Modeling, Vol 10, No. 12, pp.891-900, 1988.

[26] Peng.Li and N.U.Ahmed, On Exponential Stability of Infinite Dimensional Systems with Bounded or Unbounded Perturbations, Applicable Analysis, Vol. 30, pp 175-187, 1988.

[27] J.L. Lions and E.Magenes, Non-Homogeneous Boundary Value Problems and Applications, Vol. 1, Springer-Verlag, New York Heidelberg Berlin, 1972.

[28] N.U. Ahmed, Semigroup Theory with Applications to Systems and Control, Pitman Research Notes in Mathematics Series, 246, Longman Scientific and Technical, U.K, John Wily& Sons, Inc., New York, 1991.

[29] A.R. Mitchell and D.F. Griffiths, The Finite Difference Methods in Partial Differential Equations, John Wiley, Chichester, New York, 1980.

[30] W.A. Ames, Numerical Methods for Partial Differential Equations, Acadimic Press, New York, 1977.

[31] W. Rümelin, Numerical Treatment of Stochastic Differential Equations, SIAM Journal on Numerical Analysis, Vol. 19, pp. 604-613, 1982.

[32] N.U.Ahmed, 1998 A General Mathematical Framework for Stochastic Analysis of Suspension Bridges, Nonlinear Analysis, Series B, (To Appear).

[33] H.Harbi, 1997 Dynamic Models of Suspension Bridges and their Stabilities, Msc. Thesis, Ottawa University,Canada

[34] L.Meirovitch, Analytical Methods in Vibrations, Mc Graw-Hill, New York, 1967.

[35] Irfan Altas, Jonathan Dym, Murli M. Gupta, and Ram P. Monohar,Multigrid Solution of Automatically Generated High-Order Discretizations for the Biharmonic Equation. SIAM J. SCI. Comput. vol. 19, N0. 5, pp. 1575-1585, September 1998.

[36] J.W. Stephenson, Single cell Discretization of Order Two and Four for Biharmonic Problems, Journal of Computational Physics **55**, 65-80 (1984).

[37] Murli M. Gupta, Direct Solution of the biharmonic Equation Using Noncoupled Approach, Journal of Computational Physics **33**, 236-248 (1979).

[38] Patrick Le Tallec, Jan Mandel and Marina Vidrascu, A Neumann Domain Decomposition Algorithm for Solving Plate and Shell Problems, **I N R I A**, Institut National de Recherche en Informatique et en Automatique, Rapport de Recherche **N0. 2635**, August 1995.

[39] George Avalos and Irena Lasiecka, Boundary controllability of Thermoelastic plates via the Free Boundary conditions, SIAM J. Control Optim. Vol. 38, N0. 2, pp.337-383. 2000.

[40] S. Timochenko, D.H. Young, and W. Weaver JR., Vibration Problems in Engineering, by Jhon Wiley & Sons, Inc. 1974.

[41] Brice Carnahan, H.A. Luther and James O. Wilkes, Applied Numerical Methods, Jhon Wiley & Sons, Inc. 1969.

[42] J.L. Lions et E. Magenes, Probèmes Aux Limites Non Homogènes et Applications, Dunod , Paris, 1968

[43] J. Nečas, Les Méthodes Directes en Théorie des équations Elliptiques, Masson, Paris/Academie, Prague, 1967